Contributions of the four essential entry glycoproteins to HSV-1 tropism and the selection of entry routes.

Adam T. Hilterbrand[1], Raecliffe Daly[1,2], and Ekaterina E. Heldwein[1,2,#]

[1]Department of Molecular Biology and Microbiology, [2]Graduate Program in Cellular, Molecular, and Developmental Biology, Tufts University School of Medicine, Boston, MA 02111

#Correspondence: katya.heldwein@tufts.edu

Running title: Entry of VSV pseudotyped with HSV-1 glycoproteins

ABSTRACT

Herpes Simplex viruses (HSV-1 and HSV-2) encode up to 15 glycosylated and unglycosylated envelope proteins. Four of these, gB, gH, gL, and gD, are essential for entry and mediate cell-cell fusion when co-expressed in uninfected, receptor-bearing cells. However, their contributions to HSV-1 tropism and the selection of entry routes are unclear. To begin addressing this, we previously pseudotyped VSV lacking its native glycoprotein, G, with HSV-1 glycoproteins gB, gH, gL, and gD. This novel VSVΔG-BHLD pseudotype recapitulated several aspects of HSV-1 entry: it could enter murine C10 cells, required gB, gH, gL, gD, and a cellular receptor for entry, and was sensitive to neutralization by gB and gH/gL antibodies. Here, we screened six additional HSV-1-susceptible cell lines and found that only two, C10 and CHO-HVEM cells, reproducibly supported a receptor-dependent entry by VSVΔG-BHLD. We then compared VSVΔG-BHLD and HSV-1 entry routes into these two cell lines using a combination of chemical and genetic inhibitors of cellular uptake pathways. We discovered that the VSVΔG-BHLD pseudotype not only has a narrower tropism but also uses entry pathways different from those used by HSV-1. We conclude that while the four essential HSV-1 entry glycoproteins enable entry in certain contexts, they are insufficient for entry into any HSV-1-susceptible cell nor do they specify native HSV-1 entry routes. We hypothesize that the HSV-1 envelope proteins outside the essential four (so-called "non-essential") contribute towards the tropism and the selection of native HSV-1 entry routes. Our work draws attention to the need for systematic investigation of the HSV-1 entry mechanisms and the roles of the envelope proteins that were long considered non-essential in the selection of target cells, routes of entry, and pathogenesis.

AUTHOR SUMMARY

Different viruses enter cells by diverse routes, but how that choice is made is not always clear. Understanding the mechanisms behind these choices is vital for finding strategies to prevent viral infections. In enveloped viruses, viral proteins embedded in the envelope accomplish this task. While most enveloped viruses encode one or two envelope proteins, Herpes Simplex viruses (HSV) encode up to 15. Four of these are deemed essential for entry (gB, gH, gL, and gD) whereas the rest have been termed non-essential. While these four proteins are essential, their contributions to HSV-1 cellular tropism and entry pathways have not been fully elucidated. Here, we generated virions that have only the four essential HSV-1 glycoproteins on their surface. We show that the VSVΔG-BHLD pseudotype has a narrower tropism than HSV-1 and uses different entry pathways. Thus, the four essential HSV-1 entry glycoproteins alone do not define HSV-1 tropism or specify native entry routes. We hypothesize that the HSV-1 envelope proteins outside the essential four may contribute towards tropism and entry route selection. Our work emphasizes the need to investigate the roles of the so-called non-essential envelope proteins in HSV entry. This is important because HSV enters natural target cells, epithelial cells and neurons, by different, poorly defined routes. Mechanistic understanding of HSV entry is essential for understanding its pathogenesis and developing new strategies to prevent HSV entry and spread.

55 **INTRODUCTION**

56 All viruses must enter cells to initiate infection, and different viruses accomplish this task by
57 different mechanisms: some penetrate cells at the plasma membrane while others hijack host
58 endocytic pathways. Enveloped viruses – those in which the nucleocapsid is surrounded by a
59 cell-derived lipid bilayer – penetrate the cells by merging their lipid envelopes with a cellular
60 membrane, either the plasma membrane or the membrane of an endocytic vesicle following
61 endocytosis (Fig 1) [reviewed in (1, 2)]. Viruses typically have preferred entry routes, the choice
62 of which is not always clear, and some enter different target cells by different routes.
63 Understanding what routes viruses use to enter cells and how they select them may help inform
64 strategies to prevent viral infections.

65 Herpes Simplex viruses (HSV-1 and HSV-2) are enveloped alphaherpesviruses that infect
66 much of the world's population for life, causing a panoply of diseases ranging from painful to
67 life-threatening (3, 4). An enduring mystery of HSV entry is how and why the virus enters
68 different cells by different routes: direct fusion with the plasma membrane [e.g., neurons, Vero
69 cells, Hep2 cells, reviewed in (5)] or by endocytosis and subsequent fusion with the endosomal
70 membrane [e.g., keratinocytes, corneal epithelial cells (6, 7)].

71 HSV-1 encodes 15 viral envelope proteins, 12 glycosylated and three unglycosylated
72 [reviewed in (8, 9)]. HSV-1 entry by any route requires the coordinated efforts of four
73 glycoproteins – gB, gH, gL, and gD, which are termed essential with regard to entry (10-12) –
74 and a cellular gD receptor [reviewed in (5, 13, 14)]. Binding of gD to one of its three cellular
75 receptors, nectin-1, herpesvirus entry mediator (HVEM), or 3-O-sulfated heparan sulfate (3-OS-
76 HS) (15-17), is thought to activate the conserved heterodimer gH/gL (18, 19). In turn, gH/gL
77 presumably interacts with and activates gB (20, 21), the conserved fusogen that mediates the

78 fusion of the viral envelope with the cellular membrane [reviewed in (13, 14)]. The remaining 11
79 envelope proteins encoded by HSV-1 are incorporated into virions (9) and contribute to
80 replication by aiding in egress (22) and immune evasion (23, 24), in addition to entry [reviewed
81 in (8)].

82 In addition to being required for entry, gB, gH, gL, and gD are also sufficient for cell-cell
83 fusion of uninfected receptor-bearing cells expressing these four glycoproteins (25, 26).
84 However, until recently, it was unknown whether these four glycoproteins were sufficient for
85 entry. To begin addressing this question, we previously generated VSV lacking its native
86 glycoprotein G and pseudotyped with HSV-1 gB, gH, gL, and gD through *trans*-
87 complementation, which we refer to as the VSVΔG-BHLD pseudotype (27). The VSVΔG-
88 BHLD pseudotype efficiently entered C10 cells (B78 murine melanoma cells expressing nectin-
89 1), and its entry recapitulated several important features of HSV-1 entry into susceptible cells,
90 namely, the requirement for gB, gH, gL, gD, and a gD receptor, as well as sensitivity to anti-gB
91 and anti-gH/gL neutralizing antibodies (27). However, this study left unclear whether the
92 VSVΔG-BHLD pseudotype could enter any HSV-1 susceptible cell types or specify native entry
93 routes.

94 Here, we expanded our studies to six additional HSV-1 susceptible cell lines. We found
95 that unlike HSV-1, VSVΔG-BHLD reproducibly entered only two cell lines, C10 and CHO-
96 HVEM, by non-native routes. Therefore, although the four essential HSV-1 entry glycoproteins
97 alone can mediate entry in certain contexts, they do not enable entry into any HSV-1-susceptible
98 cell and do not specify native entry routes. Differences in tropism and routes of entry could not
99 be accounted for by either cell-surface receptor levels, their nature (nectin-1 vs. HVEM), the
100 relative amounts of gB, gH, gL, and gD, virion morphology (VSV vs. HSV-1), or some other

101 aspect of VSV biology. Therefore, we hypothesize that the so-called non-essential HSV-1
102 envelope proteins, which are missing from the VSVΔG-BHLD pseudotype, are important in
103 specifying both HSV-1 tropism and its routes of cell entry.
104
105 **RESULTS**
106 ***VSVΔG-BHLD pseudotypes enter a limited repertoire of HSV-1 susceptible cells.*** To determine
107 the tropism of the VSVΔG-BHLD pseudotype, we selected several commonly used HSV-1-
108 susceptible cell lines, including four primate cell lines, HeLa, HaCaT, Vero, and SH-SY5Y, and
109 three derivatives of rodent cell lines B78H1 (mouse) and CHO-K1 (hamster) engineered to
110 stably express human nectin-1 [B78H1-nectin-1 (C10) and CHO-nectin-1] or HVEM (CHO-
111 HVEM) (28, 29). Parental B78H1 and CHO-K1 cell lines served as receptor-negative controls.
112 As expected, HSV-1 entered all receptor-bearing cells but not receptor-negative B78H1 or CHO-
113 K1 cells (Fig 2A). VSVΔG-BHLD pseudotype also readily infected C10 cells but not parent
114 B78H1 cells (Fig 2B), consistent with previous observations (27). VSVΔG-BHLD pseudotype
115 also infected CHO-HVEM and CHO-nectin-1 cells in a receptor-dependent manner albeit with
116 much lower efficiency (Fig 2B). However, no measurable infection by the VSVΔG-BHLD
117 pseudotype was observed with HeLa, HaCaT, Vero, or SH-SY5Y cells (Fig 2B) even at MOI of
118 10 (S1 Fig).
119 To rule out contributions of VSV particle morphology, cells were also infected with two
120 VSV pseudotype controls, VSVΔG-G and VSVΔG-PIV5. VSVΔG-G is VSVΔG pseudotyped *in*
121 *trans* with native VSV glycoprotein G and is known to enter susceptible cells by a clathrin-
122 mediated endocytosis (CME) (30). VSVΔG-PIV5 is VSVΔG pseudotyped with entry
123 glycoproteins HN and F from parainfluenza virus 5 (PIV5), which enters susceptible cells by

124 fusion at the plasma membrane (31) just as PIV5 itself. Both VSVΔG-G and VSVΔG-PIV5
125 pseudotypes infected all 9 tested cell lines, with varying efficiency (Fig 2C, D), which suggested
126 that limited tropism of VSVΔG-BHLD pseudotype cannot be explained by VSV particle
127 morphology or some other aspect of VSV biology.
128
129 ***Narrow tropism of VSVΔG-BHLD pseudotypes cannot be fully accounted for by variations in***
130 ***cell surface receptor levels.*** Levels of HSV-1 gD receptors nectin-1 and HVEM vary across cell
131 lines, and susceptibility to HSV-1 infection generally correlates with surface receptor levels (29).
132 To investigate the role of relative cell surface levels of HSV-1 receptors in VSVΔG-BHLD
133 tropism, we measured the amount of nectin-1 and HVEM on the surface of B78H1, C10, CHO-
134 K1, CHO-nectin-1, CHO-HVEM, HeLa, HaCaT, Vero, and SH-SY5Y cells by flow cytometry
135 (Fig 3). As expected, neither receptor was detected on the receptor-negative cell lines B78H1 and
136 CHO-K1 (Figs 3A, B). C10 and HaCaT cells had the highest levels of nectin-1 whereas
137 intermediate levels of nectin-1 were detected on CHO-nectin-1, HeLa, Vero and SH-SY5Y cells
138 (Fig 3A). As expected, CHO-HVEM cells had high levels of HVEM but no detectable nectin-1
139 on their surface (Fig 3B). In addition to nectin-1, HaCaT, HeLa, and Vero cells also had HVEM
140 on their surfaces (Fig 3B) albeit in low amounts, which suggested that in these cells, nectin-1
141 likely functions as the primary receptor. Surprisingly, while both C10 and HaCaT cells express
142 high levels of nectin-1, the VSVΔG-BHLD pseudotype efficiently enters only C10 cells.
143 To correlate VSVΔG-BHLD entry with receptor levels more directly, CHO-K1 cells were
144 transfected with a plasmid encoding either nectin-1 or HVEM. Cell surface levels of either
145 receptor increased with increasing amounts of transfected DNA. While VSVΔG-BHLD entry
146 increased with increasing amounts of nectin-1 DNA, entry maxed out in cells transfected with 10

147 ng of DNA at around 2%, similar to entry levels observed in the CHO-nectin-1 cell line (~3%).
148 Additionally, the level of receptor detected in cells transfected with 10 ng of plasmid DNA and
149 the level of receptor in CHO-nectin-1 stable cells are very similar, and support similar levels of
150 entry (~2% vs. 3% infected cells, respectively). However, increased nectin-1 expression did not
151 result in increased VSVΔG-BHLD entry (S2 Fig). CHO-K1 cells transfected with a plasmid
152 expressing HVEM showed increasing surface expression of the receptor with increasing amounts
153 of DNA but never reached expression levels of the CHO-HVEM stable cell line. While HVEM
154 levels did increase, a similar increase in VSVΔG-BHLD entry was not observed. Together these
155 results suggest that while VSVΔG-BHLD entry requires a gD receptor, neither its surface
156 expression levels, nor its type can account for the narrow tropism of the VSVΔG-BHLD
157 pseudotype.
158
159 ***Differences in HSV-1 and VSVΔG-BHLD tropisms cannot be attributed to differences in the***
160 ***relative amounts of glycoproteins gB, gH, gL, and gD.*** We next tested whether differences in
161 relative amounts of gB, gH, gL, and gD on HSV-1 vs. VSVΔG-BHLD pseudotype could account
162 for the stark differences in tropism. Purified HSV-1 and VSVΔG-BHLD particles were analyzed
163 for the gB, gH, gL, and gD content by Western blot (Fig 4A), and relative gB:gH:gL:gD ratios
164 were determined by densitometry. In each virus, levels of gH, gL, and gD were normalized to
165 gB. We observed no statistically significant differences in the relative amounts of gH, gL, or gD
166 between HSV-1 and VSVΔG-BHLD virions (Fig 4B), and their ratios were very similar. We
167 conclude that the differences in the relative amounts of gB, gH, gL, and gD in HSV-1 or
168 VSVΔG-BHLD virions do not account for the differences in tropism.
169

170 ***Entry of both VSVΔG-BHLD and HSV-1 into C10 and CHO-HVEM cells occurs by***
171 ***endocytosis.*** HSV-1 enters different cell lines either by fusion at the plasma membrane or by
172 endocytosis [(32, 33); reviewed in (5)]. As far as the cells used in the present study, HSV-1
173 enters C10, CHO-nectin-1, CHO-HVEM, HeLa, and HaCaT cells by endocytosis (7, 32, 34) and
174 Vero and SH-SY5Y cells, by fusion at the plasma membrane (7, 33). To determine how the
175 VSVΔG-BHLD pseudotype enters C10 and CHO-HVEM cells, we first treated cells with a
176 hypertonic solution of sucrose, a broad inhibitor of endocytic pathways (35, 36). Entry of both
177 HSV-1 and VSVΔG-BHLD into C10 and CHO-HVEM cells was inhibited by sucrose (Fig 5A,
178 B, E, F) and, thus, occurs by endocytosis, just as entry of HSV-1.
179 As a control, sucrose also prevented the endocytic uptake of Alexa Fluor 488-labeled
180 transferrin into both C10 and CHO-HVEM cells (Fig 5I). As expected, sucrose did not inhibit
181 entry of VSVΔG-PIV5 into either cell line because PIV5 enters by fusion at the plasma
182 membrane (31), thus serving as a negative control (Fig 5D, H). Entry of VSV occurs by an
183 endocytic route (37-39), and, accordingly, sucrose blocked entry of VSVΔG-G into C10 cells
184 (Fig 5C). Surprisingly, it did not block entry into CHO-HVEM cells (Fig 5G), suggesting that the
185 inhibitory effect of hypertonic sucrose on VSV-G-dependent entry may be cell-type specific.
186
187 ***VSVΔG-BHLD entry requires dynamin but not clathrin whereas HSV-1 entry requires both.***
188 Having established that the VSVΔG-BHLD pseudotype entered cells by endocytosis, we next
189 sought to identify its entry mechanism and systematically compare it to that of HSV-1. To do
190 this, we used a combination of chemical and genetic means of inhibiting different cellular
191 proteins involved in various endocytic uptake pathways (Fig 1). In most cases, two to three

192 inhibitors per pathway were selected to establish the involvement of a particular pathway with
193 greater confidence (40) and to rule out potential unintended effects of the inhibitors.
194 First, we examined the role of the clathrin-mediated endocytosis (CME), one of the most
195 well studied and highly used endocytic pathways hijacked by viruses for entry [reviewed in (2,
196 41)]. CME requires both clathrin, a triskelion-shaped protein that assembles cage-like structures
197 underneath the plasma membrane to promote receptor-mediated endocytosis (42), and a GTPase
198 dynamin that mediates scission of the endocytic vesicle (43). We chose three commonly used
199 dynamin inhibitors: Dynasore, Dyngo-4a, and myristyltrimethylammonium bromide (MiTMAB).
200 Dynasore and Dyngo-4a inhibit dynamin GTPase activity, which is necessary for dynamin-
201 mediated membrane fission (35), whereas MiTMAB binds the membrane-interacting pleckstrin
202 homology (PH) domain of dynamin and prevents dynamin association with the membrane (44).
203 As a clathrin inhibitor, we chose Pitstop-2, which selectively blocks CME by preventing ligand
204 association with the clathrin terminal domain (35). Another CME inhibitor, chlorpromazine,
205 which prevents clathrin association with the plasma membrane (35), was also tested. However, at
206 previously published inhibitory concentrations, chlorpromazine was toxic to both C10 and CHO-
207 HVEM cells, judging by the altered cellular morphology. Inhibitory activity of all four
208 compounds was ascertained by their ability to inhibit CME of transferrin (Figs 6E and 7I).
209 HSV-1 entry into both C10 and CHO-HVEM cell lines was inhibited by all four
210 inhibitors (Figs 6A, C and 7A, E) indicating that HSV-1 enters both cell lines by CME. While
211 entry of VSVΔG-BHLD pseudotypes into C10 and CHO-HVEM cells was sensitive to all
212 dynamin inhibitors (Fig 6B, D), surprisingly, Pitstop-2 did not block VSVΔG-BHLD entry (Fig
213 7B, F), which ruled out CME as the entry mechanism. Collectively, these observations suggested
214 that HSV-1 enters both C10 and CHO-HVEM cells by CME whereas VSVΔG-BHLD

215 pseudotypes utilize a dynamin-dependent, clathrin-independent entry route. These results were
216 the first indication of possible differences in entry routes of HSV-1 and VSVΔG-BHLD.
217 As expected, entry of VSVΔG-G into C10 cells was blocked by all three dynamin
218 inhibitors and the clathrin inhibitor (Fig 7C and S3A Fig), confirming previous reports of VSV
219 entry into other cell types by CME (30, 39). Like C10 cells, VSVΔG-G entry into CHO-HVEM
220 cells was blocked by Pitstop-2 (Fig 7G). However, its entry into CHO-HVEM cells was only
221 blocked by two of the dynamin inhibitors, Dynasore and Dyngo-4a, and not by MiTMAB (S3C
222 Fig). Given the results that two of the dynamin inhibitors and clathrin inhibition blocked
223 VSVΔG-G entry into CHO-HVEM cells, it is likely that the entry mechanism is CME. In
224 contrast, VSVΔG-PIV5 entry into CHO-HVEM cells was not blocked by any of the four
225 inhibitors (Fig 7H and S3D Fig), consistent with the previous report of entry into other cell types
226 by fusion at the plasma membrane (31). Surprisingly, VSVΔG-PIV5 entry into C10 cells was
227 blocked by Dyngo-4a (S3B Fig), hinting at a potential role for dynamin in PIV5 entry into C10
228 cells. However, given that neither the other dynamin inhibitors, Dynasore and MiTMAB, nor
229 Pitstop-2 blocked entry (Fig 7H and S3B Fig), Dyngo-4a may be blocking VSVΔG-PIV5 entry
230 by an off-target effect.
231
232 ***Cholesterol is important for entry of both HSV-1 and VSVΔG-BHLD.*** Given that VSVΔG-
233 BHLD entry into both C10 and CHO-HVEM cells did not require clathrin, we next evaluated
234 contributions of known clathrin-independent endocytic (CIE) mechanisms. Caveolin-dependent
235 endocytosis is a major CIE route (45) that is hijacked by viruses such as SV40 or Japanese
236 encephalitis virus (46, 47). Caveolin-1 is cellular protein that, similarly to clathrin, promotes
237 membrane curvature and subsequent endocytosis through the formation of caveolae (48).

238 Caveolin-dependent entry requires plasma membrane cholesterol for proper caveolin-1
239 association with the membrane (48, 49).
240 Entry of both HSV-1 and VSVΔG-BHLD into C10 and CHO-HVEM cells decreased
241 when cholesterol was removed from cellular membranes using a cholesterol-depleting agent,
242 methyl-β-cyclodextrin (MβCD) (Fig 8A-D). Efficiency of cholesterol depletion was confirmed
243 by showing that association of cholera toxin subunit B (CTB) with C10 and CHO-HVEM cells,
244 which is dependent on membrane cholesterol (50), was decreased with MβCD treatment (S4F
245 Fig). Entry of VSVΔG-G was insensitive to cholesterol depletion (S4A, C Fig), as observed in
246 other cell types (51, 52). By contrast, cholesterol was important for VSVΔG-PIV5 entry into C10
247 cells (S4B Fig) but not into CHO-HVEM cells (S4D Fig), suggesting that the role of cellular
248 cholesterol in PIV5 entry is cell-type dependent.
249 Entry of neither HSV-1 nor VSVΔG-BHLD into CHO-HVEM cells was reduced by the
250 knockdown of caveolin-1 (Fig 8E), similarly to the VSVΔG-G and VSVΔG-PIV5 (53) control
251 viruses (S4E Fig). Successful knockdown was verified by western blot (Fig 8F). Surprisingly, no
252 caveolin-1 was detected in C10 cells (Fig 8G). To rule out species-dependent recognition of
253 murine vs. hamster caveolin-1, 3T12 cells (murine fibroblasts) were tested for the presence of
254 caveolin-1. Indeed, caveolin-1 was detected in 3T12 cells (Fig 8G), confirming that C10 cells
255 express no detectable caveolin-1. We conclude that cellular cholesterol plays an important role in
256 the entry of both HSV-1 and VSVΔG-BHLD but that neither virus utilizes caveolin-1-mediated
257 endocytosis for entry into C10 and CHO-HVEM cells.
258
259 ***Neither HSV-1 nor VSVΔG-BHLD utilize macropinocytosis for entry, but NHE1 and Rac1 are***
260 ***important for VSVΔG-BHLD entry in a cell-dependent manner.*** We next evaluated the

261 potential involvement of macropinocytosis, another common endocytic viral entry pathway. We
262 selected three known inhibitors of macropinocytosis: the actin filament disruptor cytochalasin D
263 (CytoD), the Na^+/H^+-exchange (NHE) inhibitor 5-(N-Ethyl-N-isopropyl)amiloride (EIPA), and
264 the Rac1 inhibitor NSC23766 (35). EIPA blocks macropinocytosis by blocking Na^+/H^+ exchange
265 proteins (NHE), which decreases the intracellular pH and inhibits small GTPase function
266 important for macropinocytosis (54). NSC23766 blocks macropinocytosis by inhibiting the
267 activity of the small GTPase Rac1 (55). Inhibitory activity of all three compounds was confirmed
268 by their ability to inhibit macropinocytosis of rhodamine-B-labeled 70-kDa dextran (Fig 9E).
269 HSV-1 entry into either C10 or CHO-HVEM cells was not appreciably inhibited by any
270 of the macropinocytosis inhibitors (Fig 9A, C). By contrast, VSVΔG-BHLD entry was reduced
271 by NSC23766 and, to a lesser extent, EIPA (though not statistically significant) in both C10 and
272 CHO-HVEM cells but not by cytochalasin D (Fig 9B, D). While the inhibitory effect of the
273 NSC23766 and EIPA would appear to implicate macropinocytosis as the route of VSVΔG-
274 BHLD entry into C10 and CHO-HVEM cells, the lack of actin involvement argues against it.
275 This is because assembly of filamentous actin is essential for the formation of membrane ruffles
276 during macropinocytosis (56) and is, thus, the major hallmark of macropinocytosis (57). Without
277 actin polymerization, cells cannot support fluid phase uptake processes such as
278 macropinocytosis. Likewise, we did not observe any appreciable co-localization of the VSVΔG-
279 BHLD particles with 70 kDa rhodamine B labeled dextran, a fluid phase uptake marker (S5 and
280 S6 Figs). Taken together, our results suggest that neither HSV-1 nor VSVΔG-BHLD utilize
281 macropinocytosis for entry into C10 or CHO-HVEM cells. Efficient VSVΔG-BHLD entry,
282 however, requires NHE and Rac1 activity in both cell lines, and we hypothesize that these
283 proteins play a role in VSVΔG-BHLD entry independently of their role in macropinocytosis.

284 Although VSV enters cells by CME rather than macropinocytosis, it has been shown to
285 require filamentous actin to achieve full engulfment of the viral particle by the plasma membrane
286 during endocytosis (30). Indeed, VSVΔG-G entry into C10 cells was modestly reduced by
287 cytochalasin D and EIPA but not NSC23766 (S7A Fig) whereas its entry into CHO-HVEM cells
288 was somewhat reduced by EIPA but not cytochalasin D or NSC23766 (S7C Fig). As VSVΔG-
289 PIV5 fuses at the plasma membrane, its entry was not blocked with any of the three inhibitors of
290 macropinocytosis, and, in fact, was increased in the presence of EIPA in C10 cells (S7B, D Fig).
291
292 ***HSV-1 and VSVΔG-BHLD differ in their requirements for Rab GTPases for entry.*** Endocytic
293 entry by many viruses also requires small GTPases known as Rabs. Rab GTPases are important
294 for the formation of specific endosomal compartments in the cell (58). Given that different
295 viruses penetrate endocytic membranes at distinct endosomal maturation stages – for example,
296 VSV fuses with membranes of early endosomes whereas influenza A virus fuses with
297 membranes of late endosomes (59) – proper formation of these endosomal compartments is
298 essential for viral entry. GTPases Rab5 and Rab7 are important for the maturation and formation
299 of early endosomes and late endosomes/multi-vesicular bodies (MVBs), respectively (60).
300 Overexpression of dominant negative (DN) forms of either Rab5 (Rab5DN) or Rab7 (Rab7DN)
301 suppress early and late endosome formation, respectively (61, 62).
302 To identify the endosomal compartment(s) required for HSV-1 or VSVΔG-BHLD entry,
303 C10 and CHO-HVEM cells were transfected with fluorescently tagged Rab5DN or Rab7DN
304 expression constructs and then infected. Overexpression of either Rab5DN or Rab7DN did not
305 significantly reduce HSV-1 entry into either cell line (Fig 10A, E) or entry of VSVΔG-BHLD
306 into CHO-HVEM cells (Fig 10F). However, VSVΔG-BHLD entry into C10 cells was reduced in

307 the presence of Rab5DN and, to a lesser extent, Rab7DN (Fig 10B). These results suggest that
308 HSV-1 entry into both cell lines and VSVΔG-BHLD entry into CHO-HVEM cells are either
309 independent of the endosomal maturation state or occur very early after internalization, prior to
310 the formation of early or late endosomes. By contrast, VSVΔG-BHLD likely enters the cytosol
311 of C10 cells out of early endosomes. This observation marked the first instance of a difference in
312 VSVΔG-BHLD entry into C10 vs. CHO-HVEM cells.

313 As expected, entry of VSVΔG-G into both C10 and CHO-HVEM cells was reduced in
314 the presence of Rab5DN (Fig 10C, G), in accordance with reports of VSV fusing with
315 membranes of early endosomes (39). VSVΔG-PIV5 entry into C10 cells was insensitive to either
316 Rab5DN or Rab7DN (Fig 10D). While VSVΔG-PIV5 entry into CHO-HVEM cells was reduced
317 by both Rab5DN and Rab7DN in a statistically significant manner (Fig 10H), the differences
318 between mean values were less than 10%. Therefore, Rab5DN and Rab7DN have a minimal
319 effect on VSVΔG-PIV5 entry as expected for a virus that fuses with the plasma membrane.
320

321 ***Small GTPase Arf6 regulates entry of HSV-1 but not VSVΔG-BHLD.*** Another small GTPase,
322 ADP-ribosylation factor 6 (Arf6), which is involved in regulating vesicular trafficking (63),
323 regulates the endocytic entry of HIV, Coxsackievirus, and Vaccinia virus (40, 64, 65). To probe
324 the role of Arf6 in entry, cells were treated with NAV-2729, which blocks Arf6 interaction with
325 guanine exchange factors (GEFs) thereby preventing its activation (66). HSV-1 entry into both
326 C10 and CHO-HVEM cells was inhibited by NAV-2729 (Fig 11A, E) whereas VSVΔG-BHLD
327 entry into either cell line was not inhibited, which suggests that HSV-1 entry requires Arf6
328 activity but entry of VSVΔG-BHLD does not (Fig 11B, F).

329 As anticipated, VSVΔG-PIV5 entry was not inhibited by NAV-2729 in either C10 or
330 CHO-HVEM cells (Fig 11D, H). However, VSVΔG-G entry was inhibited by NAV-2729 in both
331 C10 and CHO-HVEM cells, suggesting that Arf6 could be involved in VSV endocytosis (Fig
332 11C, G). These results point to a previously unappreciated role of Arf6 in HSV-1 and VSV entry.
333
334 ***Entry of VSVΔG-BHLD pseudotype requires endosomal acidification in a cell-dependent***
335 ***manner.*** As HSV-1 and VSVΔG-BHLD enter cells by endocytosis, we assessed the role of
336 endosomal acidification in entry. Previous work showed that HSV-1 entry into CHO-HVEM
337 cells was sensitive to inhibitors of endosomal acidification ammonium chloride (NH_4Cl) and
338 monensin (32), and thus likely required endosomal acidification. Conversely, HSV-1 entry into
339 C10 cells was insensitive to either NH_4Cl or bafilomycin A1 (BFLA), another inhibitor of
340 endosomal acidification (34).
341 To investigate the role of endosomal acidification in entry, we used BFLA, NH_4Cl, and
342 monensin. All three inhibitors effectively blocked endosomal acidification as evidenced by
343 decrease in Lysotracker fluorescence in inhibitor-treated cells (Fig 12E). VSVΔG-G, which
344 requires low pH as a trigger for membrane fusion during endocytic entry, was sensitive to all
345 three inhibitors (S8A, C Fig). In contrast, VSVΔG-PIV5, which enters cells by fusion at the
346 plasma membrane, was insensitive to any of the inhibitors (S8B, D Fig).
347 HSV-1 entry into C10 cells was inhibited by NH_4Cl and monensin but not by BFLA (Fig
348 12A), the latter in agreement with a previous report (34). HSV-1 entry into CHO-HVEM cells
349 was inhibited by NH_4Cl and monensin, which was consistent with the previous report (32), but
350 not by BFLA (Fig 12C). VSVΔG-BHLD entry into C10 cells was inhibited by all three

351 endosomal acidification inhibitors (Fig 12B) whereas VSVΔG-BHLD entry into CHO-HVEM
352 cells was inhibited only by NH_4Cl (Fig 12D).
353 Although HSV-1 entry into C10 and CHO-HVEM cells was sensitive to NH_4Cl and
354 monensin, the lack of inhibition in the presence of BFLA, an endosomal V-ATPase inhibitor (Fig
355 1), suggests that the effects of NH_4Cl and monensin on HSV-1 entry may be independent of their
356 effects on endosomal acidification. VSVΔG-BHLD entry into C10 cells was sensitive to all three
357 endosomal acidification inhibitors and likely depends on endosomal acidification. Finally,
358 VSVΔG-BHLD entry into CHO-HVEM cells could only be inhibited by NH_4Cl and is unlikely
359 to require endosomal acidification. We hypothesize that the discrepancy in the inhibitory effects
360 among the three inhibitors could potentially be due to the distinct mechanisms by which BFLA,
361 NH_4Cl, and monensin raise endosomal pH.
362
363 **DISCUSSION**
364 Decades of research have established glycoproteins gB, gH, gL, and gD as essential for HSV-1
365 entry (10-12). These four glycoproteins are also sufficient for cell-cell fusion when co-expressed
366 in uninfected, receptor-bearing cells (25, 26). While these studies greatly increased our
367 understanding of the HSV-1 entry and fusion mechanisms, the specific contributions of these
368 four glycoproteins to cellular tropism and the selection of entry routes remain incompletely
369 understood in part due to the presence of 11 other proteins in the HSV-1 envelope. To begin
370 addressing this, we utilized a VSV-based pseudotype containing HSV-1 gB, gH, gL, and gD.
371 Being devoid of other HSV-1 proteins, the VSVΔG-BHLD pseudotype provided a deconvoluted
372 platform to identify contributions of the core set of four essential glycoproteins to HSV-1 cellular
373 tropism and the selection of entry routes.

374 Previously, we showed that the VSVΔG-BHLD pseudotype efficiently entered C10 cells
375 and that its entry recapitulated several important features of HSV-1 entry into susceptible cells:
376 the requirement for gB, gH, gL, gD, and a gD receptor, and sensitivity to anti-gB and anti-gH/gL
377 neutralizing antibodies (27). Here, we expanded this study to six additional HSV-1-susceptible
378 cell lines and found that out of seven, only C10 and CHO-HVEM cells supported appreciable
379 VSVΔG-BHLD entry. We then showed that the VSVΔG-BHLD pseudotype entered these two
380 cell lines by different mechanisms as judged by the differences in sensitivity to endocytic
381 inhibitors (Fig 13). Therefore, while gB, gH, gL, and gD are sufficient for entry in certain
382 contexts, they do not enable entry into any HSV-1-susceptible cell type and do not specify native
383 entry routes. We hypothesize that the so-called non-essential HSV-1 envelope proteins contribute
384 towards the tropism and the selection of entry routes, likely, in a cell-specific manner.
385
386 ***VSVΔG-BHLD pseudotype has a narrower cellular tropism than HSV-1.*** HSV-1 can infect a
387 wide range of receptor-bearing cell lines and types from many different species (8). By contrast,
388 VSVΔG-BHLD had a narrower tropism, efficiently entering only 2 out of 7 cell lines used.
389 Puzzlingly, the VSVΔG-BHLD pseudotype entered two engineered rodent cell lines but none of
390 the four human and primate cell lines typically used in HSV-1 studies, HeLa, Vero, HaCaT, or
391 SH-SY5Y even at MOI of 10. The lack of VSVΔG-BHLD entry did not correlate with the HSV-
392 1 entry route into these cells, endocytosis in HeLa and HaCaT (7, 32) vs. plasma membrane in
393 Vero and SH-SY5Y (7, 33). The reasons for the observed differences in tropism are yet unclear
394 but do not appear to be due to differences in ratios of gB, gH, gL, and gD or VSV biology.
395 Therefore, we hypothesize that the narrower tropism of VSVΔG-BHLD is instead due to the
396 absence of one or more of the 11 HSV-1 envelope proteins outside of the core set of four.

397 Indeed, some of these proteins have been shown to increase HSV-1 entry efficiency. For
398 example, deletion of glycoprotein K (gK) significantly reduced HSV-1 entry into Vero cells (67).
399 Another HSV-1 glycoprotein, gC, aids viral attachment by binding heparan sulfate moieties of
400 cell surface proteoglycans (68) and promotes efficient entry into cells that HSV-1 enters by an
401 endocytic route (69). Thus, it is plausible that HSV-1 glycoproteins outside of the core set of four
402 could modulate HSV-1 entry efficiency by tuning the cellular tropism of the virus. In other
403 words, the more efficiently HSV-1 enters a given cell type, the more likely that cell type is to be
404 successfully infected.
405
406 ***VSVΔG-BHLD pseudotype is internalized differently from HSV-1.*** If HSV-1 gB, gH, gL, and
407 gD were sufficient to specify the native routes of HSV-1 entry, then we would have expected the
408 VSVΔG-BHLD pseudotype to utilize the same entry routes into C10 and CHO-HVEM as HSV-
409 1. Indeed, entry of both viruses occurred by endocytosis, required dynamin and cellular
410 cholesterol, and was independent of caveolin-1 or actin polymerization. However, further
411 investigation showed that the entry requirements of VSVΔG-BHLD ultimately differed from
412 those of HSV-1 in several regards (Fig 13).
413 Unlike HSV-1 entry, VSVΔG-BHLD entry was insensitive to the clathrin inhibitor
414 Pitstop-2, which implicated CIE, rather than CME, as the entry route. Macropinocytosis is a CIE
415 used by a number of viruses. But while VSVΔG-BHLD entry into both C10 and CHO-HVEM
416 cells was sensitive to two inhibitors of macropinocytosis, EIPA and NSC23766, it was
417 insensitive to the inhibitor of actin polymerization, cytochalasin D. Given the central role of actin
418 polymerization in macropinocytosis (57), these data suggest that macropinocytosis is not the
419 primary entry mechanism for VSVΔG-BHLD pseudotype. Indeed, VSVΔG-BHLD particles did

420 not colocalize with a fluid phase uptake marker 70 kDa rhodamine B labeled dextran to an
421 appreciable extent.
422 If the VSVΔG-BHLD pseudotype does not enter cells by macropinocytosis, why is its
423 entry sensitive to EIPA and NSC23766? One possibility is that their respective targets, Na^+/H^+
424 exchangers and Rac1, could contribute to VSVΔG-BHLD entry by regulating, for example, the
425 function of other cellular GTPases (54) or other downstream targets of Rac1 [reviewed in (70)].
426 An alternative possibility is that EIPA inhibits VSVΔG-BHLD entry due to its previously
427 described pleiotropic effect manifested as gross reorganization of the endosomal network and
428 changes in Na^+ and H^+ gradients in the cell (71, 72). Similarly, inhibition of Rac1 by NSC23766
429 could have a pleotropic effect because Rac1, in addition to its roles in regulating the actin
430 cytoskeleton, is also involved in several other cellular processes (73).
431
432 ***VSVΔG-BHLD pseudotype and HSV-1 differ in late-stage entry requirements.*** Many viruses
433 that enter by endocytosis, for example, influenza A and VSV, rely on Rab-GTPase-dependent
434 endosomal maturation and endosomal acidification (59). VSVΔG-BHLD entry into C10 cells
435 required Rab5, a marker of the early endosomes, and endosomal acidification. Conversely,
436 VSVΔG-BHLD entry into CHO-HVEM cells required neither Rab5, nor Rab7, nor endosomal
437 acidification. Entry of HSV-1 into both C10 and CHO-HVEM cells appeared independent of
438 Rab5, Rab7, or endosomal acidification, similar to VSVΔG-BHLD entry into CHO-HVEM cells.
439 While both Rab5 and Rab7 appeared disposable for HSV-1 entry into either cell line, Arf6, a
440 small GTPase involved in endosomal trafficking including CME and CIE (63), may play a role.
441 How Arf6 promotes HSV-1 entry is yet unclear, considering its numerous downstream effectors,
442 including lipid modifying enzymes, proteins involved in endosome trafficking, and GTPase

443 activating proteins (GAPs) and guanine exchange factors (GEFs) for other GTPases [reviewed in
444 (63)]. Interestingly, Arf6 did not seem important for VSVΔG-BHLD entry.

445 Surprisingly, we observed that HSV-1 entry into both C10 and CHO-HVEM cells was
446 insensitive to BFLA yet inhibited by NH_4Cl and monensin. While BFLA specifically blocks
447 endosomal acidification by inhibiting endosomal V-ATPase proton pumps, NH_4Cl and monensin
448 can also affect other cellular processes, e.g., vacuolization or organelle swelling. Therefore, we
449 hypothesize that HSV-1 entry into either the C10 or the CHO-HVEM cells does not require
450 endosomal acidification. Sensitivity of HSV-1 entry to NH_4Cl and monensin could, instead, be
451 due to their ability to interfere with other cellular processes. Both compounds alter ion content of
452 the endosomes and cause vacuolization (74), so a change in endosomal ion concentration may
453 reduce the ability of HSV-1 to fuse with the endosomal membrane. Indeed, binding of HSV-1 to
454 the cell surface releases intracellular Ca^{2+} stores (75) and increases intracellular levels of Cl^- ions
455 (76), both of which appear important for subsequent entry.

456 One notable difference between VSVΔG-BHLD and HSV-1 entry into C10 cells was the
457 apparent reliance on endosomal acidification of the former but not of the latter virus. Previous
458 work suggested that HSV-1 entry into C10 cells does not require endosomal acidification (34).
459 Indeed, we found that HSV-1 entry into C10 cells was insensitive to inhibition by bafilomycin
460 A1 (BFLA). However, VSVΔG-BHLD entry into C10 cells was blocked by BFLA treatment.

461 Putting these results together, we hypothesize that HSV-1, which does not require Rab5/7
462 or endosomal acidification of entry, fuses with the endosomal membrane prior to maturation of
463 the newly formed vesicle into an early endosome [pH ~6.2 (77)] (Fig 13). This latter scenario is
464 consistent with the rapid nature of HSV-1 entry into both C10 and B78A10 cells (B78 murine
465 melanoma cells expressing HVEM) cells ($t_{1/2}$ = 8-10 minutes) (34). Alternatively, endosomal

466 maturation status does not influence HSV-1 fusion with the membrane of the endocytic vesicle.
467 VSVΔG-BHLD entry into CHO-HVEM cells, likewise, does not require Rab5/7 or endosomal
468 acidification. Therefore, it is likely that VSVΔG-BHLD fusion with the endosomal membrane
469 occurs prior to delivery of the endocytic vesicle to an early endosome. In contrast, VSVΔG-
470 BHLD entry into C10 cells requires both Rab5 and endosomal acidification. In that case, we
471 hypothesize that VSVΔG-BHLD fuses with membranes of early endosomes. This would suggest
472 that in C10 cells, other HSV-1 envelope proteins enable fusion prior to endosomal acidification.
473
474 ***Utility of the VSV-based pseudotyping approach for studying HSV-1 entry.*** The utility of the
475 VSV-based pseudotyping platform has been demonstrated on many occasions throughout the
476 years. It has been used to study the entry mechanisms of several BSL-4 pathogens (e.g. Ebola,
477 Marburg, and Junín viruses) that otherwise are limited to being studied in appropriate
478 containment facilities (78). Importantly, the entry mechanisms of these pseudotypes have been
479 shown to be similar to their respective native viruses (79), indicating that the pseudotypes
480 typically serve as useful proxies for studying the entry of the respective native viruses. Unlike
481 other pseudotypes and their respective native viruses, VSVΔG-BHLD pseudotype does not
482 mimic HSV-1 entry. We hypothesize that this is due to the lack of other envelope proteins that
483 may influence cellular tropism and entry pathways. However, other possibilities should also be
484 considered.
485 While neither particle morphology nor the ratio of gB, gH, gL, and gD appear to account
486 for the differences in HSV-1 vs. VSVΔG-BHLD entry, the differences in the lipid composition
487 may do so. VSV and HSV-1 acquire their envelopes from different sources, the plasma
488 membrane (PM) for VSV (78) vs. trans-Golgi network (TGN) or endosome-derived vesicles for

489 HSV-1 (80). Although lipidomics studies suggests that the PM, TGN, and endosomes have very
490 similar lipid composition (81), small differences in envelope lipid composition may contribute to
491 differences in entry. While interesting, this line of inquiry is beyond the scope of the present
492 study.

493 Collectively, our results implicate the so-called non-essential HSV-1 envelope proteins in
494 both the cellular tropism and the selection of viral entry routes. Previous studies have hinted at
495 the ability of some of these proteins to influence entry pathways. For example, gK is thought to
496 promote entry into neurons by fusion with the plasma membrane because deletion of the N
497 terminus of gK switches entry to endocytosis (82). gC promotes efficient endocytic entry into
498 CHO-HVEM and primary human keratinocytes (69). Other HSV-1 envelope proteins likely play
499 yet unappreciated roles in specifying tropism and influencing the selection of entry pathways,
500 potentially, in a cell-specific manner. Future studies of their contributions will not only explain
501 why HSV-1 encodes such a large number of envelope proteins but may aid in the design of better
502 strategies for blocking entry, leading to improved treatment options for HSV-1 diseases.
503

504 **METHODS**

505 ***Cells.*** HEK293T (gift from J.M. Coffin, Tufts University), Vero (ATCC® CCL-81™), HeLa
506 (ATCC® CCL-2™), and HaCaT cells (gift from J. Garlick, Tufts University) were grown in
507 Dulbecco's modified Eagle medium (DMEM; Lonza) containing high glucose, and sodium
508 pyruvate, supplemented with L-glutamine (Caisson Labs), 10% heat inactivated fetal bovine
509 serum (HI-FBS; Life Technologies) and 1X penicillin/streptomycin (pen/strep) solution
510 (Corning). B78H1 cells (a gift from R.J. Eisenberg and G.H. Cohen, University of Pennsylvania)
511 were grown in DMEM containing high glucose, sodium pyruvate, and L-glutamine

512 supplemented with 5% FBS and pen/strep solution (1X). C10 cells (a gift from R.J. Eisenberg
513 and G.H. Cohen, University of Pennsylvania), a clonal B78H1-derivative stably expressing
514 human nectin-1, were grown in DMEM containing high glucose, sodium pyruvate, and L-
515 glutamine supplemented with 5% FBS and pen/strep solution (1X) and maintained under
516 selection for nectin-1 expression with 250 μg/ml of G418 (Selleck Chemical) as done previously
517 (27). CHO-K1 cells were grown in Ham's F12 medium containing 10% FBS and pen/strep
518 solution (1X). CHO-HVEM cells, a derivative of CHO-K1 cells that stably express human
519 nectin-1, were grown in Ham's F12 medium containing 10% FBS and penicillin-streptomycin
520 solution (1X), 250 ug/ml G418 and 150 ug/ml of puromycin (AG Scientific). CHO-K1 and
521 CHO-HVEM cells were a gift from Anthony Nicola (Washington State University). SH-SY5Y
522 cells were maintained in EMEM (Sigma catalogue number) supplemented with 15% HI-FBS and
523 1X-pen/strep. SH-SY5Y cells were a kind gift from Stephen Moss (Tufts University).
524
525 ***Plasmids***. Plasmids pPEP98, pPEP99, pPEP100, and pPEP101 carry the full-length HSV-1
526 (strain KOS) genes for gB, gD, gH, and gL, respectively in a pCAGGS vector background.
527 These were kindly gifted by P.G. Spear (Northwestern University). pCMV-VSV-G, which
528 contains the full-length gene for the VSV glycoprotein, G, was a gift from J. White (University
529 of Virginia). Rab GTPase dominant negative constructs [mCherry-Rab5DN(S34N) and dsRed-
530 Rab7DN] were purchased from Addgene (61, 62). For consistency, the dsRed in dsRed-Rab7DN
531 was replaced with mCherry by amplifying mCherry with the following primers: 5'-
532 AGCGCTACCGGTCGCCACCATGGTGAGCAAGGGCGAG-3' (forward) and 5'-
533 AATTCGAAGCTTGAGCTCGAGATCTGAGCTTGTACAGCTCGTCCATGCC-3' (reverse).
534 mCherry was then cloned in frame with Rab7DN using AgeI and HindIII cut sites that were

535 engineered into the forward and reverse primers, respectively. As our HSV-1 reporter strain uses
536 tdTomato, eGFP-RabDN constructs were engineered. The same primers were used to amplify
537 eGFP from pEGFP-N2. The same cloning procedure was used to replace mCherry and dsRed
538 with eGFP in the Rab5DN and Rab7DN constructs, respectively. Isolated clones were sequenced
539 to verify mCherry and eGFP were in frame with the DN Rab genes.
540
541 ***Antibodies.*** Nectin-1 antibody [clone CK41 (83)] conjugated to phycoerythrin (PE) was
542 purchased from BD Biosciences. PE-isotype antibody was also purchased from BD Biosciences.
543 HVEM antibody (R140) was a gift from Gary Cohen (University of Pennsylvania). Caveolin-1
544 antibody (clone 4H312) was purchased from Santa Cruz Biotechnology. β-actin antibody
545 conjugated to horse radish peroxidase (HRP) was purchased from Santa Cruz Biotechnology (sc-
546 47778 HRP).
547
548 ***Chemical inhibitors***. Monensin, methyl-β-cyclodextrin, cytochalasin D, Pitstop-2, and EIPA
549 were purchased from Sigma. Dynasore and MiTMAB were purchased from Calbiochem.
550 Bafilomycin A1 was purchased from ApexBio. Ammonium chloride was purchased from Fisher
551 Scientific. Dyngo-4a was purchased from Abcam. NSC23766 was purchased from Santa Cruz
552 Biotechnology.
553
554 ***Viruses.*** Pseudotyped viral particles (VSVΔG-BHLD) were generated as described previously
555 (27). Briefly, HEK293T cells (5.5 x 10^6 cells/10 cm dish) were transfected with 2.5 μg each
556 pPEP98, pPEP99, pPEP100, and pPEP101 using polyethyleneimine (PEI at 1 mg/ml) at a 3:1
557 weight ratio of PEI to DNA. Twenty-four hours post transfection, cells were infected at an MOI

558 = 3 with VSVΔG-G (VSVΔG pseudotyped with VSV G protein). Forty-eight hours post
559 infection, supernatants were collected, cleared of cell debris (two spins at 1500xg for 10 minutes
560 each), and stored at -80 °C. VSVΔG-BHLD titers were determined on C10 cells.
561 HSV-1 (GS3217, F strain) was kindly provided by G. Smith (Northwestern University).
562 HSV-1 was propagated on Vero cells and titers were determined by plaque assay on Vero cells
563 as previously described (HSV textbook). VSVΔG-G helper virus was generated by M. Whitt (U.
564 Tennessee) and kindly provided by J. White (U. of Virginia). New stocks were generated
565 similarly to the VSVΔG-BHLD pseudotypes, replacing the HSV-1 glycoproteins with pCMV-
566 VSV-G (10 μg per 10 cm dish). VSVΔG-G titers were determined on C10 cells. VSVΔG-PIV5
567 was generated and kindly provided by S.P.J. Whelan (HMS). As VSVΔG-PIV5 contains the
568 PIV5 HN and F proteins in the VSV genome, no complementation *in trans* was necessary.
569 VSVΔG-PIV5 was grown on HEK293T cells and titers were determined on C10 cells.
570
571 ***Entry experiments.*** 3 x 10^5 B78H1, C10, CHO-K1, CHO-HVEM, HeLa, HaCaT, Vero, or SH-
572 SY5Y cells were seeded in 35 mm dishes. Cells were infected with viruses at a MOI=1. Viruses
573 were incubated with cells at 37 °C for one hour. After one hour, viruses that had not entered were
574 inactivated with a low pH wash (40 mM Na-citrate, 10 mM KCl, 135 mM NaCl, pH 3.0).
575 Complete growth media was added back to cells and infections were allowed to progress for six
576 hours prior to analysis by flow cytometry. Entry experiments in the presence of inhibitors were
577 performed similarly except that prior to infection, C10 and CHO-HVEM cells were pretreated
578 with the indicated inhibitors for one hour prior to infection. All inhibitors, with the exception of
579 sucrose and methyl-β-cyclodextrin, were present during the infection and the six hours post
580 infection prior to analysis by flow cytometry by measuring tdTomato expression (HSV-1

581 GS3217) or EGFP expression (VSV pseudotypes) to allow sufficient time for viral entry and
582 expression of the fluorescent reporters.
583 Viral entry experiments in the presence of fluorescently labeled Rab GTPase dominant
584 negative constructs were performed and analyzed as follows: cells infected with HSV-1
585 (tdTomato) were transfected with pEGFP-N2 as an empty vector control or eGFP-tagged RabDN
586 constructs whereas cells infected with VSV pseudotypes (eGFP) were transfected with
587 pmCherry-C1 empty vector control or mCherry-tagged RabDN constructs. The data represented
588 are the percentage of infected cells that were successfully transfected with either the empty
589 vector control or the RabDN constructs.
590 Prior to flow cytometry analysis, cells were trypsinized, resuspended in media and
591 pelleted at 450xg for five minutes. Cells were washed with 1X PBS containing 1 mM EDTA (to
592 prevent clumping). Cells were pelleted again at 450xg for five minutes. Cells were then
593 resuspended in 1X PBS with 1 mM EDTA and transferred to FACS tubes. Flow cytometry was
594 performed on a BD LSR II or FACSCalibur instrument. tdTomato expression (HSV-1 GS3217)
595 or EGFP expression (VSV pseudotypes) were measured as a proxy for viral entry. Data analysis
596 was done using FlowJo software (v. 8.8.7).
597
598 ***Analyses of nectin-1 expression and viral infectivity by flow cytometry.*** Nectin-1 was detected
599 on the surface of cells by staining them with nectin-1 antibody conjugated to PE. Briefly, 10^6
600 cells were plated into 10 cm dishes. The next day, cells were lifted from the dishes with 1X-PBS
601 containing 5 mM EDTA. Cells were then pelleted, resuspended in 300 μl FACS buffer (1X-PBS,
602 2% FBS, 1 mM EDTA), and divided evenly between microfuge tubes for mock, PE-isotype, or
603 PE-anti-nectin-1 treatment. Cells were incubated with 1 μg of antibody for 30 minutes on ice

604 with agitation every 10 minutes. After 30 minutes, cells were pelleted and washed three times
605 with FACS buffer, re-suspended, then immediately analyzed by flow cytometry (FACSCalibur).
606
607 ***Virus purification and densitometry analysis.*** HSV-1 and VSVΔG-BHLD virions were purified
608 and subjected to immunoblot for gB, gH, gL, and gD. Briefly, five T-175 flasks of Vero cells
609 were infected with HSV-1 (MOI 0.01). HSV-1 was crudely purified as previously described (84).
610 HSV-1 particles were then purified over a continuous 15-50% sucrose gradient (85). The purified
611 band of HSV-1 was collected by puncture and aspiration. VSVΔG-BHLD virions were generated
612 as previously mentioned (see *Viruses* section of Materials and Methods). VSVΔG-BHLD
613 particles were then pelleted at 20,000 RPM. VSVΔG-BHLD virions were then resuspended and
614 purified over a continuous 15-35% Optiprep gradient [protocol adapted from (86, 87)] and
615 collected by puncture and aspiration. HSV-1 and VSVΔG-BHLD virions were pelleted at
616 20,0000 RPM. Western blots for gB, gH, gL, and gD were done using the rabbit polyclonal R68
617 antibody (gB), the rabbit polyclonal R137 antibody (gH), the mouse monoclonal antibody L1
618 (gL), and the mouse monoclonal antibody R7 (gD). Secondary antibodies from LI-COR were
619 used in order to perform densitometry analysis using the Image Studio Lite software (IRDye®
620 680RD goat anti-rabbit and IRDye® 800CW goat anti-mouse). Raw densitometry values for gH,
621 gL, and gD blots were normalized to their respective raw densitometry values for gB and
622 reported as fold-differences to gB.
623
624 ***Confocal Microscopy.*** 10^5 cells (C10 and CHO-HVEM) were seeded onto 12 mm glass
625 coverslips (Chemglass) in 24 well plates. Prior to labeling cells with specific markers of different
626 endocytosis pathways, cells were pretreated with inhibitors for one hour at 37 °C. Post pre-

627 treatment, cells were chilled to 4 °C for 10-15 minutes and were subsequently incubated with
628 specific endocytic markers: Transferrin-Alexa Fluor 488 (50 μg/ml, Thermo Fisher Scientific),
629 70-kD dextran-rhodamine B (1 mg/ml, Thermo Fisher Scientific), or Lysotracker (1 μM, Thermo
630 Fisher Scientific). Cells were incubated with endocytic markers for 10 minutes at 4 C. After the
631 10-minute incubation, C10 cells were shifted to 37 °C for 10 minutes and CHO-HVEM cells
632 were shifted to 37 °C for 30 minutes (Transferrin-Alexa Fluor 488 and Lysotracker) (88) or 40
633 minutes (70 kDa dextran) (89). After incubation at 37 °C, cells were washed 3 times with 1X-
634 PBS and fixed in 4% paraformaldehyde for 15 minutes at room temperature. Cells were washed
635 three times with 1X-PBS and incubated with 2.5 μg/ml of DAPI (ThermoFisher Scientific)
636 diluted in 1X-PBS for 15 minutes at room temperature. Cells were washed again three times with
637 1X-PBS and mounted onto Prolong Gold Antifade (Life Technologies) on glass slides (Thermo
638 Fisher Scientific). Coverslips were sealed with clear nail polish and analyzed by confocal
639 microscopy using a Leica SPE microscope. Images were analyzed in Fiji (90). For 70-kDa
640 dextran and VSVΔG-BHLD co-localization experiments, C10 and CHO-HVEM cells were
641 incubated with 1 mg/ml 70 kDa dextran and VSVΔG-BHLD (MOI = 1) for 1 hour at 4 C to
642 allow for virion attachment. Cells were then shifted to 37 C for 20 minutes. After 20 minutes,
643 cells were prepared for confocal microscopy by fixing with 4% paraformaldehyde, permeabilized
644 and blocked with 1X PBS containing 5% normal goat serum and 0.3% Triton X-100. Cells were
645 then incubated with anti-gB antibody (R68) overnight at 4 C. The next day, cells were incubated
646 with a secondary antibody labeled with FITC for 1 hour at room temperature. Slides were then
647 prepared as described above.
648

649 ***siRNA-mediated knockdown.*** Mouse caveolin-1 siRNA, and a control siRNA were purchased
650 from Santa Cruz Biotechnologies. 50 pmol of siRNA (0.625 μg) (cav-1 or scramble [scr]) were
651 diluted into 100 μl of Optimem. In another tube, 3.125 μl of PEI (1 mg/ml) was diluted into 100
652 μl of Optimem. The diluted PEI was mixed with the diluted siRNA to a final ratio of 5:1 (w:w)
653 of PEI to siRNA and incubated at room temperature for 30 minutes. The complex was added
654 dropwise to CHO-HVEM cells plated in 35 mm dishes (3 x 10^5 cells/dish). Cells were incubated
655 at 37 °C for 48 hours before infection and subsequent flow cytometry analysis.
656

657 **ACKNOWLEDGEMENTS**

658 We thank Stephen Kwok and Allen Parmelee at the Tufts Laser Cytometry Core facility for their
659 help with FACS experiments; Roselyn Eisenberg and Gary Cohen (University of Pennsylvania)
660 for the gifts of antibodies and cell lines; Sean Whelan (Washington University) for the gift of
661 VSVΔG-PIV5 pseudotype; Anthony Nicola (Washington State University) for the gift of CHO-
662 HVEM cells; Richard Longnecker (Northwestern University) for the gift of CHO-nectin-1 cells;
663 Michael Forgac (Tufts University) for the gift of Lysotracker reagent; and Michael Whitt
664 (University of Tennessee) for the gift of the VSVΔG-GFP pseudotyping platform. FACS
665 experiments were performed at the Tufts Laser Cytometry Core facility.

666 **FIGURE LEGENDS**

667 **Fig. 1. Viruses utilize diverse entry pathways.** Viruses, including HSV-1, can penetrate cells
668 by many different routes (underlined). These entry routes can be inhibited by chemical or genetic
669 means (red). Clathrin-mediated endocytosis: hypertonic sucrose, dynamin inhibitors, clathrin
670 inhibitors. Caveolin-mediated endocytosis: siRNA against caveolin-1, cholesterol removing
671 agents. Macropinocytosis: NHE inhibitor, Rac1 inhibitor, actin polymerization inhibition.
672 GTPase Arf6: block interactions with GEFs via chemical inhibitor. Endosomal compartment
673 formation (early or late): Rab5 dominant negative (DN) and Rab7DN, respectively. Endosomal
674 acidification: V-ATPase proton pump inhibition, weak base, or carboxylic ionophore.

675

676 **Fig. 2. VSVΔG-BHLD pseudotype has a narrower cellular tropism than HSV-1.** HSV-1
677 (A), VSVΔG-BHLD (B), VSVΔG-G (C), and VSVΔG-PIV5 (D) entry was assessed on nine cell
678 lines, B78H1, C10, CHO-K1, CHO-nectin-1, CHO-HVEM, HeLa, Vero, HaCaT, and SH-SY5Y.
679 Cells were infected at a MOI of 1. Entry was quantitated by flow cytometry at 6 hours post
680 infection.

681

682 **Fig. 3. Cell surface levels of gD receptors nectin-1 and HVEM vary across cell lines.** Cell
683 surface expression of nectin-1 (A) and HVEM (B) was analyzed by flow cytometry. Surface
684 levels of nectin-1 were quantitated by staining cells with an anti-nectin-1 monoclonal antibody
685 CK41 conjugated to phycoerythrin (PE) (green histograms). Surface levels of HVEM were
686 quantitated by staining cells with an anti-HVEM polyclonal antibody R140 and a FITC-labeled
687 secondary antibody (cyan). Blue histograms are isotype controls. Red histograms are mock (no
688 antibody) controls.

689

690 **Fig. 4. Glycoproteins gB, gH, gL, and gD are present in similar ratios in HSV-1 and**
691 **VSVΔG-BHLD pseudotypes.** HSV-1 and VSVΔG-BHLD virions were purified either through
692 a continuous sucrose gradient (HSV-1) or continuous Optiprep gradient (VSVΔG-BHLD),
693 pelleted, and analyzed for their glycoprotein content (gB, gH, gL, and gD) by Western blot (anti-
694 gB pAb R68, anti-gH pAb = R137, anti-gL mAb L1, and anti-gD pAb R7). A) A representative
695 Western blot is shown. B) The amounts of gB, gH, gL, and gD in three different virion
696 preparations were determined by densitometry. Levels of gH, gL, and gD were normalized to gB
697 levels from their respective virions. A Student's T-test with Welch's correction was used to
698 determine the significance of differences between relative amounts of gH, gL, or gD between
699 HSV-1 and VSVΔG-BHLD virions (ns = not significant; $p < 0.05$ = *; $p < 0.01$ = **; $p < 0.001$
700 = ***).

701

702 **Fig. 5. HSV-1 and VSVΔG-BHLD enter cells by endocytosis.** C10 (A-D) and CHO-HVEM
703 (E-H) cells were pretreated with a hypertonic solution of sucrose (0.3 M) and infected with HSV-
704 1, VSVΔG-BHLD, VSVΔG-G, or VSVΔG-PIV5 at MOI = 1. Infectivity was quantitated by
705 flow cytometry at 6 hours post infection. Significance was calculated using a two-tailed
706 Student's T-test with Welch's correction ($p < 0.05$ = *; $p < 0.01$ = **; $p < 0.001$ = ***). I) C10
707 and CHO-HVEM cells were pretreated with 0.3 M sucrose and incubated with 50 ug/ml of
708 AF488-labeled transferrin. Cells were fixed, counterstained with DAPI, and imaged by confocal
709 microscopy. Scale bar = 25 μm.

710

711 **Fig. 6. Both HSV-1 and VSVΔG-BHLD require dynamin for entry.** C10 (A and B) and
712 CHO-HVEM (C and D) cells were pretreated with dynamin inhibitors Dynasore (80 μM),
713 Dyngo-4a (25 μM), or MiTMAB (5 μM) and infected with HSV-1 or VSVΔG-BHLD at MOI =
714 1. Infectivity was quantitated by flow cytometry at 6 hours post infection. CHO-HVEM cells
715 treated with Dyngo-4a or MiTMAB used the same DMSO control, as indicated by the same bar
716 graph appearing twice each in panels C and D. Significance was calculated using a two-tailed
717 Student's T-test with Welch's correction ($p < 0.05$ = *; $p < 0.01$ = **; $p < 0.001$ = ***). E) C10
718 and CHO-HVEM cells were pretreated with dynamin inhibitors Dynasore, Dyngo-4a, and
719 MiTMAB at the same concentrations as in panels A-D and then incubated with 50 μg/ml of
720 AF488-labeled transferrin. Cells were fixed, counterstained with DAPI, and imaged by confocal
721 microscopy. Scale bar = 25 μm.
722
723 **Fig. 7. HSV-1 but not VSVΔG-BHLD entry requires clathrin.** C10 (A-D) and CHO-HVEM
724 (E-H) cells were pretreated with an inhibitor of clathrin-mediated endocytosis Pitstop2 (30 μM)
725 and infected with HSV-1, VSVΔG-BHLD, VSVΔG-G, or VSVΔG-PIV5 at MOI = 1. Infectivity
726 was quantitated by flow cytometry at 6 hours post infection. Significance was calculated using a
727 two-tailed Student's T-test with Welch's correction ($p < 0.05$ = *; $p < 0.01$ = **; $p < 0.001$ =
728 ***). E) C10 or CHO-HVEM cells were pre-treated with 30 μM Pitstop-2 and incubated with 50
729 μg/ml of AF488-labeled transferrin. Cells were fixed, counterstained with DAPI, and imaged by
730 confocal microscopy. Scale bar = 25 μm.
731
732 **Fig. 8. HSV-1 and VSVΔG-BHLD entry requires cellular cholesterol but not caveolin-1.**
733 C10 (A and B) and CHO-HVEM (C and D) cells were pretreated with a cholesterol-removal

734 drug methyl-β-cyclodextran, MβCD (5 mM) and infected with HSV-1 or VSVΔG-BHLD at
735 MOI = 1. Infectivity was quantitated by flow cytometry at 6 hours post infection. E) CHO-
736 HVEM cells were transfected with a caveolin-1 siRNA (cav-1) or a scrambled control siRNA
737 (scr) (both 50 pm) and infected with HSV-1 or VSVΔG-BHLD at MOI = 1. Infectivity was
738 quantitated by flow cytometry at 6 hours post infection. F) Western blot analyses, using antibody
739 clone 4H312 (Santa Cruz Biotechnology), of caveolin-1 knockdown in CHO-HVEM cells
740 (representative of three western blots, one from each biological replicate). G) Western blot
741 analyses, using antibody clone 4H312 (Santa Cruz Biotechnology), of caveolin-1 levels in C10,
742 CHO-HVEM, and 3T12 cells. Significance was calculated using a two-tailed Student's T-test
743 with Welch's correction ($p < 0.05$ = *; $p < 0.01$ = **; $p < 0.001$ = ***).
744
745 **Fig. 9. Neither HSV-1 nor VSVΔG-BHLD entry requires macropinocytosis.** C10 (A and B)
746 and CHO-HVEM (C and D) cells were pretreated with macropinocytosis inhibitors cytochalasin
747 D (2 μM), EIPA (25 μM), or NSC23766 (200 μM) and infected with HSV-1 or VSVΔG-BHLD
748 at MOI = 1. Infectivity was quantitated by flow cytometry at 6 hours post infection. Significance
749 was calculated using a two-tailed Student's T-test with Welch's correction (ns = not significant;
750 $p < 0.05$ = *; $p < 0.01$ = **; $p < 0.001$ = ***). E) C10 and CHO-HVEM cells were pretreated
751 with macropinocytosis inhibitors cytochalasin D, EIPA, or NSC23766 at the same concentrations
752 as in panels A-D and then incubated with 1.0 mg/ml of Rhodamine-B-labeled 70-kDa dextran.
753 Cells were fixed, counterstained with DAPI, and imaged by confocal microscopy. Scale bar = 25
754 μm.
755

756 **Fig. 10. Rab5 and Rab7 GTPases are dispensable for HSV-1 but not VSVΔG-BHLD entry.**
757 C10 (A-D) and CHO-HVEM (E-H) cells were transfected with Rab5DN, Rab7DN, or
758 appropriate empty vector controls (eGFP or mCherry), and infected with HSV-1, VSVΔG-
759 BHLD, VSVΔG-G, or VSVΔG-PIV5 at MOI = 1. Infectivity was quantitated by flow cytometry
760 at 6 hours post infection. Significance was calculated using a two-tailed Student's T-test with
761 Welch's correction ($p < 0.05$ = *; $p < 0.01$ = **; $p < 0.001$ = ***).
762
763 **Fig. 11. HSV-1 but not VSVΔG-BHLD entry requires Arf6.** C10 (A-D) and CHO-HVEM (E-
764 H) cells were pretreated with the Arf6 inhibitor NAV-2729 (25 μM) and infected with HSV-1 or
765 VSVΔG-BHLD at MOI = 1. Infectivity was quantitated by flow cytometry at 6 hours post
766 infection. Significance was calculated using a two-tailed Student's T-test with Welch's
767 correction ($p < 0.05$ = *; $p < 0.01$ = **; $p < 0.001$ = ***).
768
769 **Fig. 12. VSVΔG-BHLD but not HSV-1 entry requires endosomal acidification.** C10 (A and
770 B) and CHO-HVEM (C and D) cells were pretreated with inhibitors of endosomal acidification
771 BFLA (100 nM), NH_4Cl (50 mM), or monensin (15 μM) and infected with HSV-1 or VSVΔG-
772 BHLD at MOI = 1. Infectivity was quantitated by flow cytometry at 6 hours post infection.
773 Significance was calculated using a two-tailed Student's T-test with Welch's correction ($p < 0.05$
774 = *; $p < 0.01$ = **; $p < 0.001$ = ***). E) C10 and CHO-HVEM cells were pretreated with
775 inhibitors of endosomal acidification at the same concentrations as in panels A-D (BFLA,
776 NH_4Cl, or monensin) and then incubated with Lysotracker (1 μM). Cells were fixed,
777 counterstained with DAPI, and imaged by confocal microscopy. Scale bar = 25 μm.
778

779 **Fig. 13. Entry model of VSVΔG-BHLD and HSV-1.** A) Entry of VSVΔG-BHLD and HSV-1
780 entry into C10 and CHO-nectin-1 cells occurs by endocytosis and requires dynamin and
781 cholesterol. VSVΔG-BHLD entry into C10 and CHO-nectin-1 cells additionally requires NHE
782 and Rac1 activity whereas HSV-1 does not. VSVΔG-BHLD entry into C10 cells, but not CHO-
783 nectin-1 cells also requires Rab5 and endosomal acidification. HSV-1 does not require either
784 Rab5 or endosomal acidification for entry into either cell type. B) Table summarizing the cellular
785 molecules important for HSV-1 and VSVΔG-BHLD entry into C10 and CHO-HVEM cells.
786

787 **SUPPORTING INFORMATION**

788 **S1 Fig. Infecting cells at with VSVΔG-BHLD at a higher MOI does not increase entry to an**
789 **appreciable extent.** Receptor null (B78H1 and CHO-K1) and receptor bearing cells (C10, CHO-
790 HVEM, HeLa, Vero, HaCaT, and SH-SY5Y) were infected at MOI =1 (red) or MOI = 10
791 (purple). Entry efficiency was assessed by flow cytometry at 6 hours post infection.

792

793 **S2 Fig. Increased amounts of surface nectin-1 or HVEM do not increase VSVΔG-BHLD**
794 **entry.** CHO-K1 (receptor-null) cells were transfected with increasing amounts of plasmids
795 encoding nectin-1 (pBG38) (A) or HVEM (pSC386) (B). Surface expression was analyzed by
796 flow cytometry 24 hours post transfection. C) Cells transfected with nectin-1 or HVEM were
797 infected with VSVΔG-BHLD at MOI = 1. Entry efficiency was assessed at 6 hours post
798 infection by flow cytometry. In each panel, receptor-bearing stable cell line data (CHO-nectin-1
799 and CHO-HVEM) were inserted as points of comparison.

800

801 **S3 Fig. VSVΔG-G and VSVΔG-PIV5 differ in their dependence on dynamin for entry.** C10
802 (A and B) and CHO-HVEM (C and D) cells were pretreated with dynamin inhibitors Dynasore
803 (80 μM), Dyngo-4a (25 μM), or MiTMAB (5 μM) and infected with VSVΔG-G or VSVΔG-
804 PIV5 at a MOI of 1. Infectivity was quantitated by flow cytometry at 6 hours post infection.
805 CHO-HVEM cells treated with Dyngo-4a or MiTMAB used the same DMSO control as
806 indicated by the same bar graph appearing twice each in panels C and D. Significance was
807 calculated using a two-tailed Student's T-test with Welch's correction ($p < 0.05$ = *; $p < 0.01$ =
808 **; $p < 0.001$ = ***).

809

810 **S4 Fig. VSVΔG-G entry does not require cholesterol whereas VSVΔG-PIV5 entry requires**
811 **cholesterol in a cell-type-dependent manner.** C10 (A and B) and CHO-HVEM (C and D) cells
812 were pretreated with a cholesterol-removal drug methyl-β-cyclodextran, MβCD (5 mM) and
813 infected with VSVΔG-G or VSVΔG-PIV5 at a MOI of 1. Infectivity was quantitated by flow
814 cytometry at 6 hours post infection. (E) CHO-HVEM cells were transfected with a caveolin-1
815 siRNA (cav-1) or a scrambled control siRNA (scr) (both 50 pm) and infected with VSVΔG-G or
816 VSVΔG-PIV5 at a MOI of 1. Infectivity was quantitated by flow cytometry at 6 hours post
817 infection. Significance was calculated using a two-tailed Student's T-test with Welch's
818 correction ($p < 0.05$ = *; $p < 0.01$ = **; $p < 0.001$ = ***). F) C10 and CHO-HVEM cells were
819 treated with either a solvent control (H_2O/EtOH) or methyl-β-cyclodextrin (MβCD), then
820 incubated with cholera toxin subunit B labelled with Alexa Fluor 488. Confocal microscopy was
821 performed on the solvent control and methyl-β-cyclodextrin treated cells. Cells were fixed,
822 counterstained with DAPI, and imaged by confocal microscopy. Scale bar = 25 μm.
823
824 **S5 Fig. VSVΔG-BHLD does not co-localize with the fluid-phase marker 70 kDa dextran in**
825 **C10 cells.** C10 cells were incubated with 1 mg/ml of rhodamine-B labelled 70 kDa dextran and
826 VSVΔG-BHLD (MOI = 1) for one hour at 4˚C. Cells were then shifted to 37 ˚C for 20 minutes.
827 Cells were fixed, counterstained with DAPI, and imaged by confocal microscopy. gB was
828 detected by immunofluorescence using the rabbit pAb R68 and anti-rabbit IgG conjugated to
829 FITC. Green = gB (marker for VSVΔG-BHLD particles); Red = 70 kDa dextran. Scale bar = 25
830 μm.
831

832 **S6 Fig. VSVΔG-BHLD, in large, does not co-localized with the fluid-phase marker, 70 kDa**
833 **dextran, in CHO-HVEM cells.** CHO-HVEM cells were incubated with 1 mg/ml of rhodamine-
834 B labelled 70 kDa dextran and VSVΔG-BHLD (MOI = 1) for one hour at 4˚C. Cells were then
835 shifted to 37˚C for 20 minutes. Cells were fixed, counterstained with DAPI, and imaged by
836 confocal microscopy. gB was detected by immunofluorescence using the rabbit pAb R68 and
837 anti-rabbit IgG conjugated to FITC. Green = gB (marker for VSVΔG-BHLD particles); Red = 70
838 kDa dextran. Scale bar = 25 μm.
839
840 **S7 Fig. VSVΔG-G and VSVΔG-PIV5 entry does not require macropinocytosis.** C10 (A and
841 B) and CHO-HVEM (C and D) cells were pretreated with macropinocytosis inhibitors
842 cytochalasin D (2 μM), EIPA (25 μM), or NSC23766 (200 μM) and infected with VSVΔG-G or
843 VSVΔG-PIV5 at a MOI of 1. Infectivity was quantitated by flow cytometry at 6 hours post
844 infection. Significance was calculated using a two-tailed Student's T-test with Welch's
845 correction ($p < 0.05$ = *; $p < 0.01$ = **; $p < 0.001$ = ***).
846
847 **S8 Fig. VSVΔG-G but not VSVΔG-PIV5 entry requires endosomal acidification.** C10 (A
848 and B) and CHO-HVEM (C and D) cells were pretreated with inhibitors of endosomal
849 acidification BFLA (100 nM), NH_4Cl (50 mM), or monensin (15 μM) and infected with
850 VSVΔG-G or VSVΔG-PIV5 at MOI = 1. Infectivity was quantitated by flow cytometry at 6
851 hours post infection. Significance was calculated using a two-tailed Student's T-test with
852 Welch's correction ($p < 0.05$ = *; $p < 0.01$ = **; $p < 0.001$ = ***).
853

854 **REFERENCES**

855 1. Mas V, Melero JA. Entry of enveloped viruses into host cells: membrane fusion. Subcell
856 Biochem. 2013;68:467-87.
857 2. Mercer J, Schelhaas M, Helenius A. Virus entry by endocytosis. Annu Rev Biochem.
858 2010;79:803-33.
859 3. Steiner I, Benninger F. Update on herpes virus infections of the nervous system. Curr
860 Neurol Neurosci Rep. 2013;13(12):414.
861 4. Bradley H, Markowitz LE, Gibson T, McQuillan GM. Seroprevalence of herpes simplex
862 virus types 1 and 2--United States, 1999-2010. J Infect Dis. 2014;209(3):325-33.
863 5. Agelidis AM, Shukla D. Cell entry mechanisms of HSV: what we have learned in recent
864 years. Future Virol. 2015;10(10):1145-54.
865 6. Miranda-Saksena M, Denes CE, Diefenbach RJ, Cunningham AL. Infection and
866 Transport of Herpes Simplex Virus Type 1 in Neurons: Role of the Cytoskeleton. Viruses.
867 2018;10(2).
868 7. Nicola AV, Hou J, Major EO, Straus SE. Herpes simplex virus type 1 enters human
869 epidermal keratinocytes, but not neurons, via a pH-dependent endocytic pathway. J Virol.
870 2005;79(12):7609-16.
871 8. Karasneh GA, Shukla D. Herpes simplex virus infects most cell types in vitro: clues to its
872 success. Virol J. 2011;8:481.
873 9. Hilterbrand AT, Heldwein EE. Go go gadget glycoprotein!: HSV-1 draws on its sizeable
874 glycoprotein tool kit to customize its diverse entry routes. PLoS Pathog. 2019;15(5):e1007660.
875 10. Cai WH, Gu B, Person S. Role of glycoprotein B of herpes simplex virus type 1 in viral
876 entry and cell fusion. J Virol. 1988;62(8):2596-604.
877 11. Roop C, Hutchinson L, Johnson DC. A mutant herpes simplex virus type 1 unable to
878 express glycoprotein L cannot enter cells, and its particles lack glycoprotein H. J Virol.
879 1993;67(4):2285-97.
880 12. Ligas MW, Johnson DC. A herpes simplex virus mutant in which glycoprotein D
881 sequences are replaced by beta-galactosidase sequences binds to but is unable to penetrate into
882 cells. J Virol. 1988;62(5):1486-94.
883 13. Heldwein EE, Krummenacher C. Entry of herpesviruses into mammalian cells. Cell Mol
884 Life Sci. 2008;65(11):1653-68.
885 14. Connolly SA, Jackson JO, Jardetzky TS, Longnecker R. Fusing structure and function: a
886 structural view of the herpesvirus entry machinery. Nat Rev Microbiol. 2011;9(5):369-81.
887 15. Spear PG. Herpes simplex virus: receptors and ligands for cell entry. Cell Microbiol.
888 2004;6(5):401-10.
889 16. Carfi A, Willis SH, Whitbeck JC, Krummenacher C, Cohen GH, Eisenberg RJ, et al.
890 Herpes simplex virus glycoprotein D bound to the human receptor HveA. Mol Cell.
891 2001;8(1):169-79.
892 17. Di Giovine P, Settembre EC, Bhargava AK, Luftig MA, Lou H, Cohen GH, et al.
893 Structure of herpes simplex virus glycoprotein D bound to the human receptor nectin-1. PLoS
894 Pathog. 2011;7(9):e1002277.
895 18. Atanasiu D, Whitbeck JC, Cairns TM, Reilly B, Cohen GH, Eisenberg RJ. Bimolecular
896 complementation reveals that glycoproteins gB and gH/gL of herpes simplex virus interact with
897 each other during cell fusion. Proc Natl Acad Sci U S A. 2007;104(47):18718-23.

898 19. Avitabile E, Forghieri C, Campadelli-Fiume G. Complexes between herpes simplex virus
899 glycoproteins gD, gB, and gH detected in cells by complementation of split enhanced green
900 fluorescent protein. J Virol. 2007;81(20):11532-7.
901 20. Chowdary TK, Cairns TM, Atanasiu D, Cohen GH, Eisenberg RJ, Heldwein EE. Crystal
902 structure of the conserved herpesvirus fusion regulator complex gH-gL. Nat Struct Mol Biol.
903 2010;17(7):882-8.
904 21. Atanasiu D, Saw WT, Cohen GH, Eisenberg RJ. Cascade of events governing cell-cell
905 fusion induced by herpes simplex virus glycoproteins gD, gH/gL, and gB. J Virol.
906 2010;84(23):12292-9.
907 22. Lau SY, Crump CM. HSV-1 gM and the gK/pUL20 complex are important for the
908 localization of gD and gH/L to viral assembly sites. Viruses. 2015;7(3):915-38.
909 23. Lubinski J, Nagashunmugam T, Friedman HM. Viral interference with antibody and
910 complement. Semin Cell Dev Biol. 1998;9(3):329-37.
911 24. Jerome KR, Fox R, Chen Z, Sarkar P, Corey L. Inhibition of apoptosis by primary
912 isolates of herpes simplex virus. Arch Virol. 2001;146(11):2219-25.
913 25. Muggeridge MI. Characterization of cell-cell fusion mediated by herpes simplex virus 2
914 glycoproteins gB, gD, gH and gL in transfected cells. J Gen Virol. 2000;81(Pt 8):2017-27.
915 26. Turner A, Bruun B, Minson T, Browne H. Glycoproteins gB, gD, and gHgL of herpes
916 simplex virus type 1 are necessary and sufficient to mediate membrane fusion in a Cos cell
917 transfection system. J Virol. 1998;72(1):873-5.
918 27. Rogalin HB, Heldwein EE. Characterization of Vesicular Stomatitis Virus Pseudotypes
919 Bearing Essential Entry Glycoproteins gB, gD, gH, and gL of Herpes Simplex Virus 1. J Virol.
920 2016;90(22):10321-8.
921 28. Miller CG, Krummenacher C, Eisenberg RJ, Cohen GH, Fraser NW. Development of a
922 syngenic murine B16 cell line-derived melanoma susceptible to destruction by neuroattenuated
923 HSV-1. Mol Ther. 2001;3(2):160-8.
924 29. Krummenacher C, Baribaud F, Ponce de Leon M, Baribaud I, Whitbeck JC, Xu R, et al.
925 Comparative usage of herpesvirus entry mediator A and nectin-1 by laboratory strains and
926 clinical isolates of herpes simplex virus. Virology. 2004;322(2):286-99.
927 30. Cureton DK, Massol RH, Saffarian S, Kirchhausen TL, Whelan SP. Vesicular stomatitis
928 virus enters cells through vesicles incompletely coated with clathrin that depend upon actin for
929 internalization. PLoS Pathog. 2009;5(4):e1000394.
930 31. Robinson LR, Whelan SP. Infectious Entry Pathway Mediated by the Human
931 Endogenous Retrovirus K Envelope Protein. J Virol. 2016;90(7):3640-9.
932 32. Nicola AV, McEvoy AM, Straus SE. Roles for endocytosis and low pH in herpes simplex
933 virus entry into HeLa and Chinese hamster ovary cells. J Virol. 2003;77(9):5324-32.
934 33. Koyama AH, Uchida T. The mode of entry of herpes simplex virus type 1 into Vero cells.
935 Microbiol Immunol. 1987;31(2):123-30.
936 34. Milne RS, Nicola AV, Whitbeck JC, Eisenberg RJ, Cohen GH. Glycoprotein D receptor-
937 dependent, low-pH-independent endocytic entry of herpes simplex virus type 1. J Virol.
938 2005;79(11):6655-63.
939 35. Dutta D, Donaldson JG. Search for inhibitors of endocytosis: Intended specificity and
940 unintended consequences. Cell Logist. 2012;2(4):203-8.
941 36. Carpentier JL, Sawano F, Geiger D, Gorden P, Perrelet A, Orci L. Potassium depletion
942 and hypertonic medium reduce "non-coated" and clathrin-coated pit formation, as well as
943 endocytosis through these two gates. J Cell Physiol. 1989;138(3):519-26.

944 37. Matlin KS, Reggio H, Helenius A, Simons K. Pathway of vesicular stomatitis virus entry
945 leading to infection. J Mol Biol. 1982;156(3):609-31.
946 38. Superti F, Seganti L, Ruggeri FM, Tinari A, Donelli G, Orsi N. Entry pathway of
947 vesicular stomatitis virus into different host cells. J Gen Virol. 1987;68 (Pt 2):387-99.
948 39. Johannsdottir HK, Mancini R, Kartenbeck J, Amato L, Helenius A. Host cell factors and
949 functions involved in vesicular stomatitis virus entry. J Virol. 2009;83(1):440-53.
950 40. Mercer J, Helenius A. Vaccinia virus uses macropinocytosis and apoptotic mimicry to
951 enter host cells. Science. 2008;320(5875):531-5.
952 41. Marsh M, Helenius A. Virus entry: open sesame. Cell. 2006;124(4):729-40.
953 42. Kirchhausen T. Three ways to make a vesicle. Nat Rev Mol Cell Biol. 2000;1(3):187-98.
954 43. Singh M, Jadhav HR, Bhatt T. Dynamin Functions and Ligands: Classical Mechanisms
955 Behind. Mol Pharmacol. 2017;91(2):123-34.
956 44. Quan A, McGeachie AB, Keating DJ, van Dam EM, Rusak J, Chau N, et al. Myristyl
957 trimethyl ammonium bromide and octadecyl trimethyl ammonium bromide are surface-active
958 small molecule dynamin inhibitors that block endocytosis mediated by dynamin I or dynamin II.
959 Mol Pharmacol. 2007;72(6):1425-39.
960 45. Mayor S, Parton RG, Donaldson JG. Clathrin-independent pathways of endocytosis. Cold
961 Spring Harb Perspect Biol. 2014;6(6).
962 46. Pelkmans L, Kartenbeck J, Helenius A. Caveolar endocytosis of simian virus 40 reveals a
963 new two-step vesicular-transport pathway to the ER. Nat Cell Biol. 2001;3(5):473-83.
964 47. Xu Q, Cao M, Song H, Chen S, Qian X, Zhao P, et al. Caveolin-1-mediated Japanese
965 encephalitis virus entry requires a two-step regulation of actin reorganization. Future Microbiol.
966 2016;11:1227-48.
967 48. Williams TM, Lisanti MP. The caveolin proteins. Genome Biol. 2004;5(3):214.
968 49. de Almeida CJG. Caveolin-1 and Caveolin-2 Can Be Antagonistic Partners in
969 Inflammation and Beyond. Front Immunol. 2017;8:1530.
970 50. Chinnapen DJ, Chinnapen H, Saslowsky D, Lencer WI. Rafting with cholera toxin:
971 endocytosis and trafficking from plasma membrane to ER. FEMS Microbiol Lett.
972 2007;266(2):129-37.
973 51. Danthi P, Chow M. Cholesterol removal by methyl-beta-cyclodextrin inhibits poliovirus
974 entry. J Virol. 2004;78(1):33-41.
975 52. Dou X, Li Y, Han J, Zarlenga DS, Zhu W, Ren X, et al. Cholesterol of lipid rafts is a key
976 determinant for entry and post-entry control of porcine rotavirus infection. BMC Vet Res.
977 2018;14(1):45.
978 53. Ravid D, Leser GP, Lamb RA. A role for caveolin 1 in assembly and budding of the
979 paramyxovirus parainfluenza virus 5. J Virol. 2010;84(19):9749-59.
980 54. Koivusalo M, Welch C, Hayashi H, Scott CC, Kim M, Alexander T, et al. Amiloride
981 inhibits macropinocytosis by lowering submembranous pH and preventing Rac1 and Cdc42
982 signaling. J Cell Biol. 2010;188(4):547-63.
983 55. Gao Y, Dickerson JB, Guo F, Zheng J, Zheng Y. Rational design and characterization of
984 a Rac GTPase-specific small molecule inhibitor. Proc Natl Acad Sci U S A. 2004;101(20):7618-
985 23.
986 56. Hansen CG, Nichols BJ. Molecular mechanisms of clathrin-independent endocytosis. J
987 Cell Sci. 2009;122(Pt 11):1713-21.
988 57. Mercer J, Helenius A. Virus entry by macropinocytosis. Nat Cell Biol. 2009;11(5):510-
989 20.

990 58. Spearman P. Viral interactions with host cell Rab GTPases. Small GTPases. 2018;9(1-
991 2):192-201.
992 59. Sieczkarski SB, Whittaker GR. Differential requirements of Rab5 and Rab7 for
993 endocytosis of influenza and other enveloped viruses. Traffic. 2003;4(5):333-43.
994 60. Langemeyer L, Frohlich F, Ungermann C. Rab GTPase Function in Endosome and
995 Lysosome Biogenesis. Trends Cell Biol. 2018;28(11):957-70.
996 61. Bohdanowicz M, Balkin DM, De Camilli P, Grinstein S. Recruitment of OCRL and
997 Inpp5B to phagosomes by Rab5 and APPL1 depletes phosphoinositides and attenuates Akt
998 signaling. Mol Biol Cell. 2012;23(1):176-87.
999 62. Choudhury A, Dominguez M, Puri V, Sharma DK, Narita K, Wheatley CL, et al. Rab
1000 proteins mediate Golgi transport of caveola-internalized glycosphingolipids and correct lipid
1001 trafficking in Niemann-Pick C cells. J Clin Invest. 2002;109(12):1541-50.
1002 63. Van Acker T, Tavernier J, Peelman F. The Small GTPase Arf6: An Overview of Its
1003 Mechanisms of Action and of Its Role in Host(-)Pathogen Interactions and Innate Immunity. Int
1004 J Mol Sci. 2019;20(9).
1005 64. Garcia-Exposito L, Barroso-Gonzalez J, Puigdomenech I, Machado JD, Blanco J,
1006 Valenzuela-Fernandez A. HIV-1 requires Arf6-mediated membrane dynamics to efficiently enter
1007 and infect T lymphocytes. Mol Biol Cell. 2011;22(8):1148-66.
1008 65. Heikkila O, Susi P, Tevaluoto T, Harma H, Marjomaki V, Hyypia T, et al. Internalization
1009 of coxsackievirus A9 is mediated by {beta}2-microglobulin, dynamin, and Arf6 but not by
1010 caveolin-1 or clathrin. J Virol. 2010;84(7):3666-81.
1011 66. Yoo JH, Shi DS, Grossmann AH, Sorensen LK, Tong Z, Mleynek TM, et al. ARF6 Is an
1012 Actionable Node that Orchestrates Oncogenic GNAQ Signaling in Uveal Melanoma. Cancer
1013 Cell. 2016;29(6):889-904.
1014 67. Foster TP, Rybachuk GV, Kousoulas KG. Glycoprotein K specified by herpes simplex
1015 virus type 1 is expressed on virions as a Golgi complex-dependent glycosylated species and
1016 functions in virion entry. J Virol. 2001;75(24):12431-8.
1017 68. Tal-Singer R, Peng C, Ponce De Leon M, Abrams WR, Banfield BW, Tufaro F, et al.
1018 Interaction of herpes simplex virus glycoprotein gC with mammalian cell surface molecules. J
1019 Virol. 1995;69(7):4471-83.
1020 69. Komala Sari T, Gianopulos KA, Weed DJ, Schneider SM, Pritchard SM, Nicola AV.
1021 Herpes Simplex Virus Glycoprotein C Regulates Low-pH Entry. mSphere. 2020;5(1).
1022 70. Bid HK, Roberts RD, Manchanda PK, Houghton PJ. RAC1: an emerging therapeutic
1023 option for targeting cancer angiogenesis and metastasis. Mol Cancer Ther. 2013;12(10):1925-34.
1024 71. Fretz M, Jin J, Conibere R, Penning NA, Al-Taei S, Storm G, et al. Effects of Na+/H+
1025 exchanger inhibitors on subcellular localisation of endocytic organelles and intracellular
1026 dynamics of protein transduction domains HIV-TAT peptide and octaarginine. J Control
1027 Release. 2006;116(2):247-54.
1028 72. Gekle M, Drumm K, Mildenberger S, Freudinger R, Gassner B, Silbernagl S. Inhibition
1029 of Na+-H+ exchange impairs receptor-mediated albumin endocytosis in renal proximal tubule-
1030 derived epithelial cells from opossum. J Physiol. 1999;520 Pt 3:709-21.
1031 73. Margiotta A, Bucci C. Coordination between Rac1 and Rab Proteins: Functional
1032 Implications in Health and Disease. Cells. 2019;8(5).
1033 74. Huotari J, Helenius A. Endosome maturation. EMBO J. 2011;30(17):3481-500.

1034 75. Cheshenko N, Pierce C, Herold BC. Herpes simplex viruses activate phospholipid
1035 scramblase to redistribute phosphatidylserines and Akt to the outer leaflet of the plasma
1036 membrane and promote viral entry. PLoS Pathog. 2018;14(1):e1006766.
1037 76. Zheng K, Chen M, Xiang Y, Ma K, Jin F, Wang X, et al. Inhibition of herpes simplex
1038 virus type 1 entry by chloride channel inhibitors tamoxifen and NPPB. Biochem Biophys Res
1039 Commun. 2014;446(4):990-6.
1040 77. Scott CC, Vacca F, Gruenberg J. Endosome maturation, transport and functions. Semin
1041 Cell Dev Biol. 2014;31:2-10.
1042 78. Whitt MA. Generation of VSV pseudotypes using recombinant DeltaG-VSV for studies
1043 on virus entry, identification of entry inhibitors, and immune responses to vaccines. J Virol
1044 Methods. 2010;169(2):365-74.
1045 79. Aleksandrowicz P, Marzi A, Biedenkopf N, Beimforde N, Becker S, Hoenen T, et al.
1046 Ebola virus enters host cells by macropinocytosis and clathrin-mediated endocytosis. J Infect
1047 Dis. 2011;204 Suppl 3:S957-67.
1048 80. Owen DJ, Crump CM, Graham SC. Tegument Assembly and Secondary Envelopment of
1049 Alphaherpesviruses. Viruses. 2015;7(9):5084-114.
1050 81. Jackson CL, Walch L, Verbavatz JM. Lipids and Their Trafficking: An Integral Part of
1051 Cellular Organization. Dev Cell. 2016;39(2):139-53.
1052 82. Musarrat F, Jambunathan N, Rider PJF, Chouljenko VN, Kousoulas KG. The Amino
1053 Terminus of Herpes Simplex Virus 1 Glycoprotein K (gK) Is Required for gB Binding to Akt,
1054 Release of Intracellular Calcium, and Fusion of the Viral Envelope with Plasma Membranes. J
1055 Virol. 2018;92(6).
1056 83. Krummenacher C, Baribaud I, Sanzo JF, Cohen GH, Eisenberg RJ. Effects of herpes
1057 simplex virus on structure and function of nectin-1/HveC. J Virol. 2002;76(5):2424-33.
1058 84. Marconi P, Manservigi R. Herpes simplex virus growth, preparation, and assay. Methods
1059 Mol Biol. 2014;1144:19-29.
1060 85. Dai X, Zhou ZH. Purification of Herpesvirus Virions and Capsids. Bio Protoc.
1061 2014;4(15).
1062 86. Kim DS, Dastidar H, Zhang C, Zemp FJ, Lau K, Ernst M, et al. Smac mimetics and
1063 oncolytic viruses synergize in driving anticancer T-cell responses through complementary
1064 mechanisms. Nat Commun. 2017;8(1):344.
1065 87. Beug ST, Beauregard CE, Healy C, Sanda T, St-Jean M, Chabot J, et al. Smac mimetics
1066 synergize with immune checkpoint inhibitors to promote tumour immunity against glioblastoma.
1067 Nat Commun. 2017;8.
1068 88. Rahn E, Petermann P, Hsu MJ, Rixon FJ, Knebel-Morsdorf D. Entry pathways of herpes
1069 simplex virus type 1 into human keratinocytes are dynamin- and cholesterol-dependent. PLoS
1070 One. 2011;6(10):e25464.
1071 89. Li L, Wan T, Wan M, Liu B, Cheng R, Zhang R. The effect of the size of fluorescent
1072 dextran on its endocytic pathway. Cell Biol Int. 2015;39(5):531-9.
1073 90. Schindelin J, Arganda-Carreras I, Frise E, Kaynig V, Longair M, Pietzsch T, et al. Fiji: an
1074 open-source platform for biological-image analysis. Nat Methods. 2012;9(7):676-82.
1075

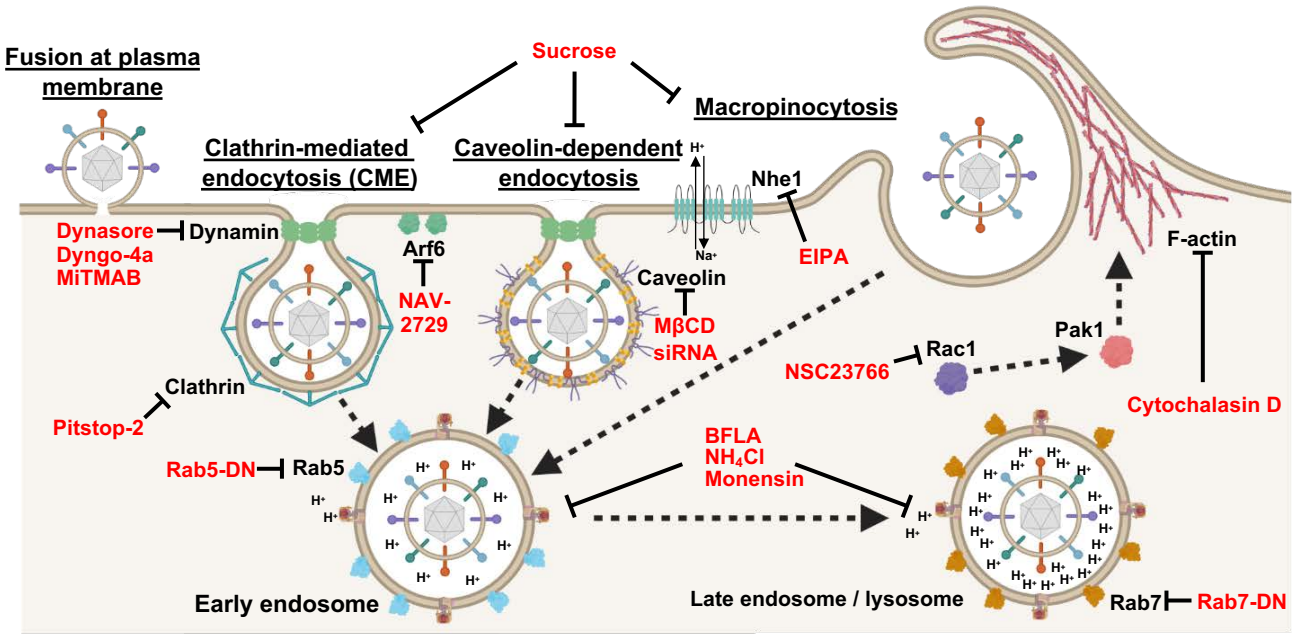

Fig. 1. Viruses utilize diverse entry pathways. Viruses, including HSV-1, can penetrate cells by many different routes (underlined). These entry routes can be inhibited by chemical or genetic means (red). Clathrin-mediated endocytosis: hypertonic sucrose, dynamin inhibitors, clathrin inhibitors. Caveolin-mediated endocytosis: siRNA against caveolin-1, cholesterol removing agents. Macropinocytosis: NHE inhibitor, Rac1 inhibitor, actin polymerization inhibition. GTPase Arf6: block interactions with GEFs via chemical inhibitor. Endosomal compartment formation (early or late): Rab5 dominant negative (DN) and Rab7DN, respectively. Endosomal acidification: V-ATPase proton pump inhibition, weak base, or carboxylic ionophore.

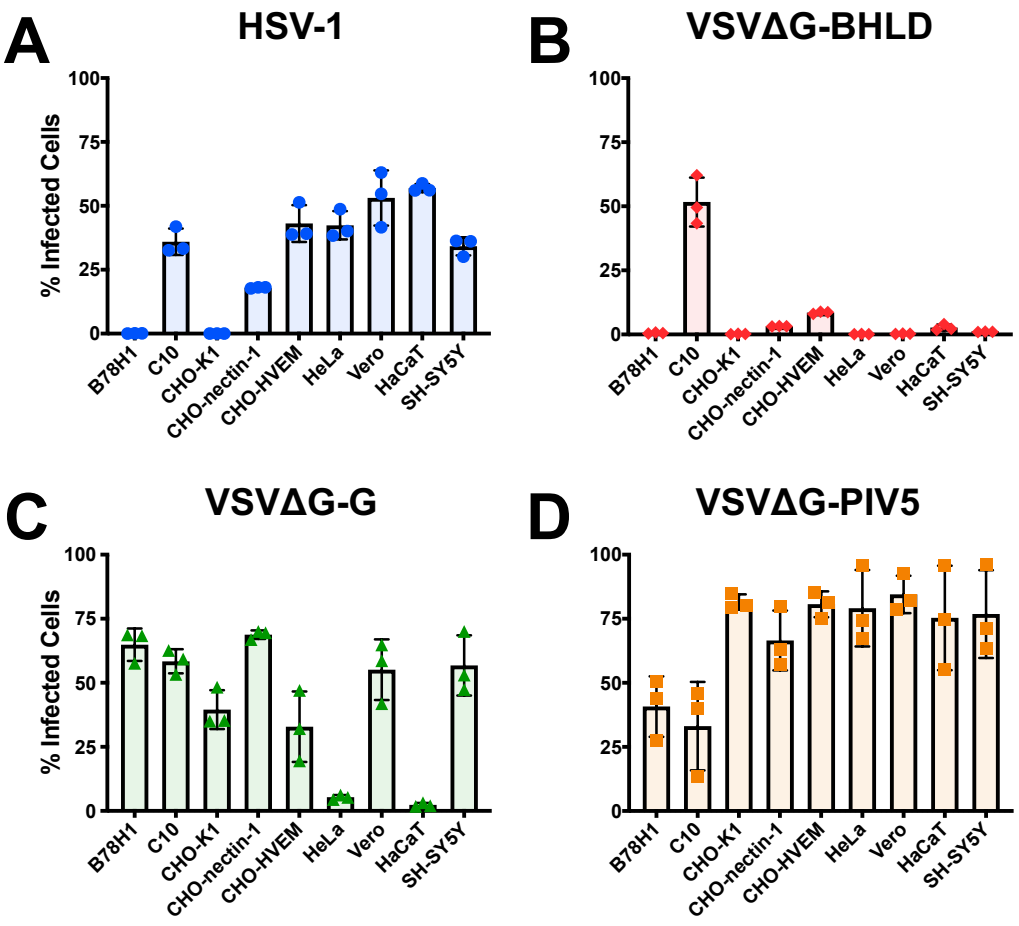

Fig. 2. VSVΔG-BHLD pseudotype has a narrower cellular tropism than HSV-1. HSV-1 (A), VSVΔG-BHLD (B), VSVΔG-G (C), and VSVΔG-PIV5 (D) entry was assessed on nine cell lines, B78H1, C10, CHO-K1, CHO-nectin-1, CHO-HVEM, HeLa, Vero, HaCaT, and SH-SY5Y. Cells were infected at a MOI of 1. Entry was quantitated by flow cytometry at 6 hours post infection.

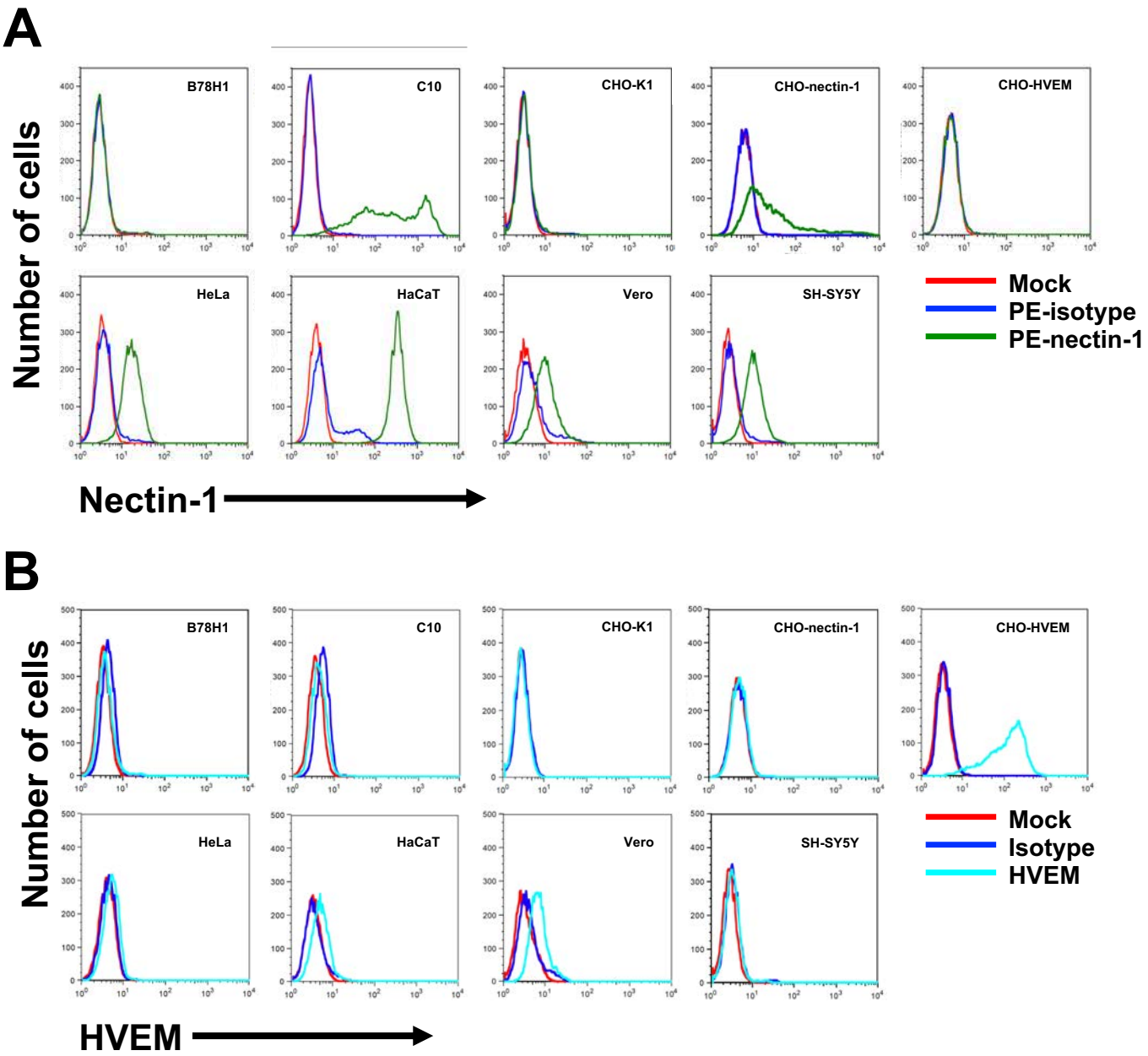

Fig. 3. Cell surface levels of gD receptors nectin-1 and HVEM vary across cell lines. Cell surface expression of nectin-1 (A) and HVEM (B) was analyzed by flow cytometry. Surface levels of nectin-1 were quantitated by staining cells with an anti-nectin-1 monoclonal antibody CK41 conjugated to phycoerythrin (PE) (green histograms). Surface levels of HVEM were quantitated by staining cells with an anti-HVEM polyclonal antibody R140 and a FITC-labeled secondary antibody (cyan). Blue histograms are isotype controls. Red histograms are mock (no antibody) controls.

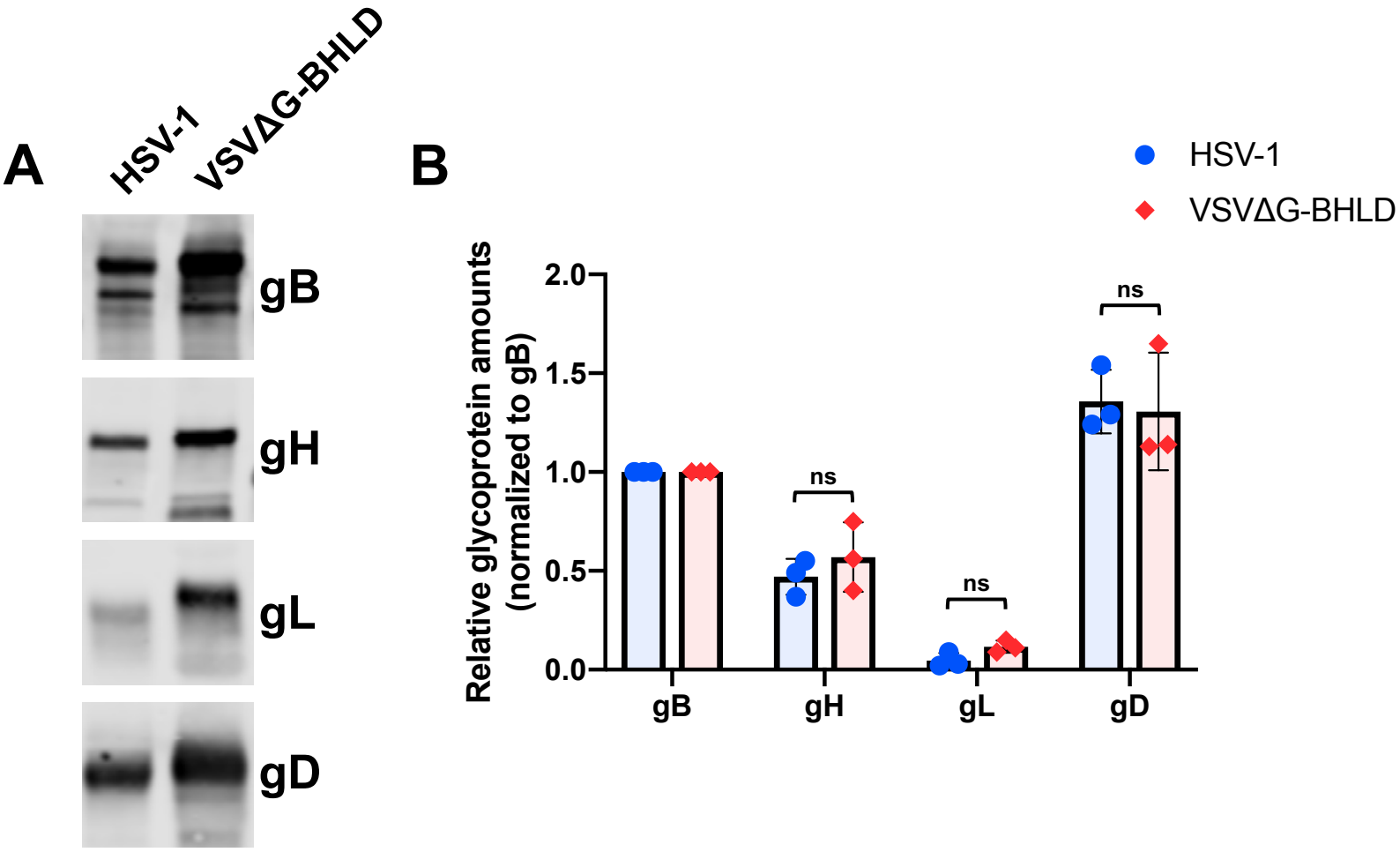

Fig. 4. Glycoproteins gB, gH, gL, and gD are present in similar ratios in HSV-1 and VSVΔG-BHLD pseudotypes. HSV-1 and VSVΔG-BHLD virions were purified either through a continuous sucrose gradient (HSV-1) or continuous Optiprep gradient (VSVΔG-BHLD), pelleted, and analyzed for their glycoprotein content (gB, gH, gL, and gD) by Western blot (anti-gB pAb R68, anti-gH pAb = R137, anti-gL mAb L1, and anti-gD pAb R7). A) A representative Western blot is shown. B) The amounts of gB, gH, gL, and gD in three different virion preparations were determined by densitometry. Levels of gH, gL, and gD were normalized to gB levels from their respective virions. A Student's T-test with Welch's correction was used to determine the significance of differences between relative amounts of gH, gL, or gD between HSV-1 and VSVΔG-BHLD virions (ns = not significant; $p < 0.05$ = *; $p < 0.01$ = **; $p < 0.001$ = ***).

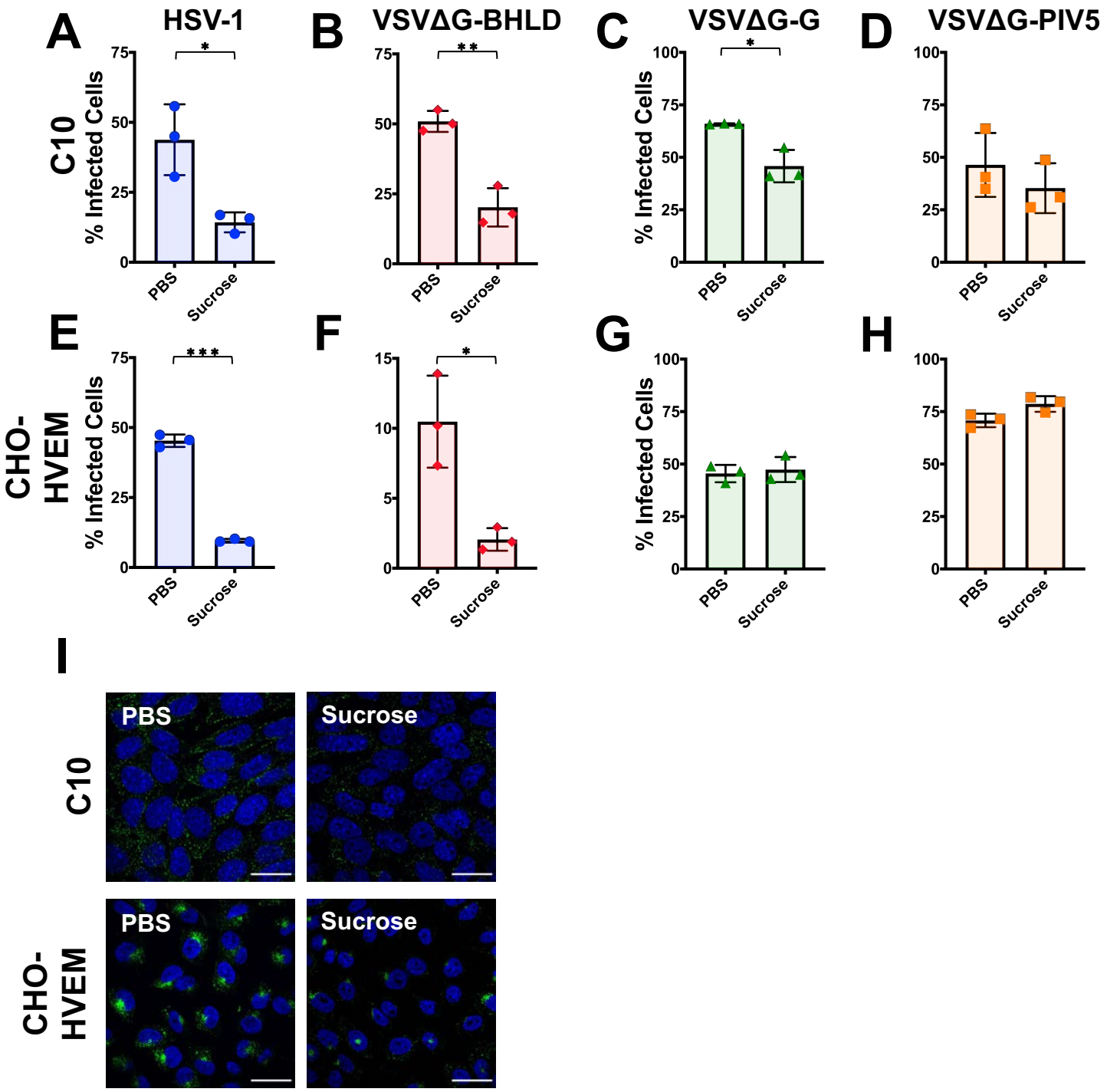

Fig. 5. HSV-1 and VSVΔG-BHLD enter cells by endocytosis. C10 (A-D) and CHO-HVEM (E-H) cells were pretreated with a hypertonic solution of sucrose (0.3 M) and infected with HSV-1, VSVΔG-BHLD, VSVΔG-G, or VSVΔG-PIV5 at MOI = 1. Infectivity was quantitated by flow cytometry at 6 hours post infection. Significance was calculated using a two-tailed Student's T-test with Welch's correction ($p < 0.05$ = *; $p < 0.01$ = **; $p < 0.001$ = ***). I) C10 and CHO-HVEM cells were pretreated with 0.3 M sucrose and incubated with 50 ug/ml of AF488-labeled transferrin. Cells were fixed, counterstained with DAPI, and imaged by confocal microscopy. Scale bar = 25 μm.

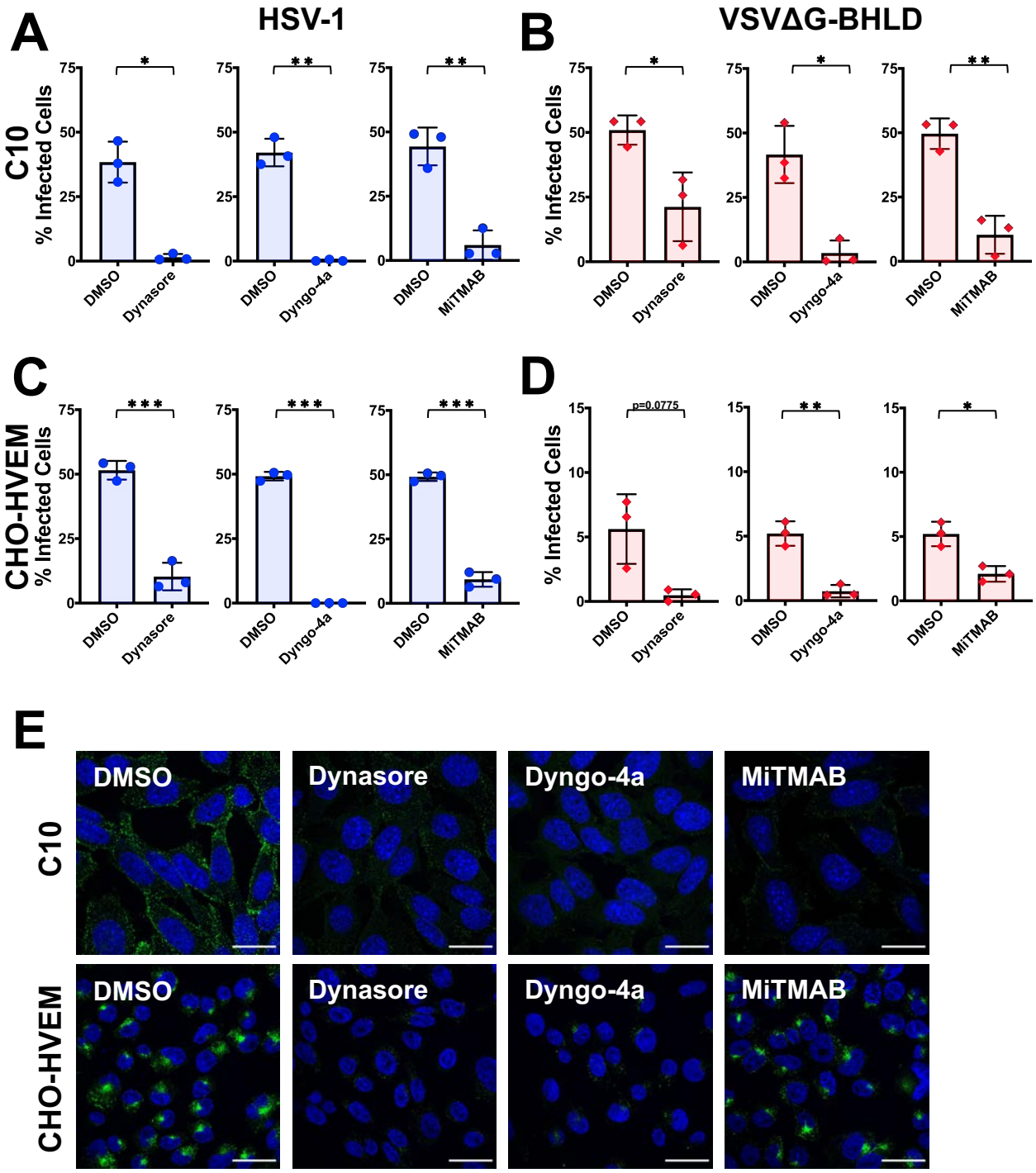

Fig. 6. Both HSV-1 and VSVΔG-BHLD require dynamin for entry. C10 (A and B) and CHO-HVEM (C and D) cells were pretreated with dynamin inhibitors Dynasore (80 μM), Dyngo-4a (25 μM), or MiTMAB (5 μM) and infected with HSV-1 or VSVΔG-BHLD at MOI = 1. Infectivity was quantitated by flow cytometry at 6 hours post infection. CHO-HVEM cells treated with Dyngo-4a or MiTMAB used the same DMSO control, as indicated by the same bar graph appearing twice each in panels C and D. Significance was calculated using a two-tailed Student's T-test with Welch's correction ($p < 0.05$ = *; $p < 0.01$ = **; $p < 0.001$ = ***). E) C10 and CHO-HVEM cells were pretreated with dynamin inhibitors Dynasore, Dyngo-4a, and MiTMAB at the same concentrations as in panels A-D and then incubated with 50 μg/ml of AF488-labeled transferrin. Cells were fixed, counterstained with DAPI, and imaged by confocal microscopy. Scale bar = 25 μm.

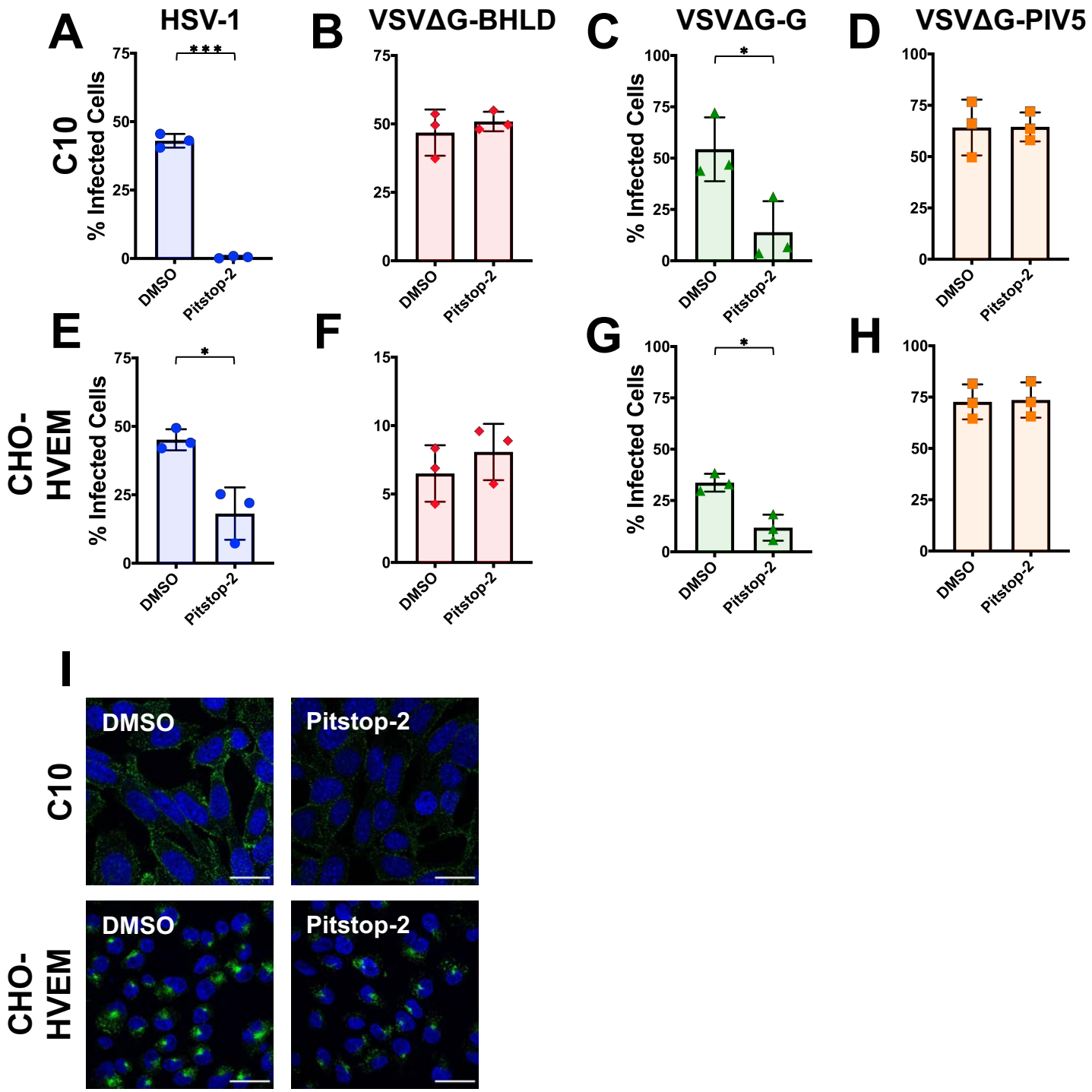

Fig. 7. HSV-1 but not VSVΔG-BHLD entry requires clathrin. C10 (A-D) and CHO-HVEM (E-H) cells were pretreated with an inhibitor of clathrin-mediated endocytosis Pitstop2 (30 μM) and infected with HSV-1, VSVΔG-BHLD, VSVΔG-G, or VSVΔG-PIV5 at MOI = 1. Infectivity was quantitated by flow cytometry at 6 hours post infection. Significance was calculated using a two-tailed Student's T-test with Welch's correction ($p < 0.05$ = *; $p < 0.01$ = **; $p < 0.001$ = ***). E) C10 or CHO-HVEM cells were pre-treated with 30 μM Pitstop-2 and incubated with 50 μg/ml of AF488-labeled transferrin. Cells were fixed, counterstained with DAPI, and imaged by confocal microscopy. Scale bar = 25 μm.

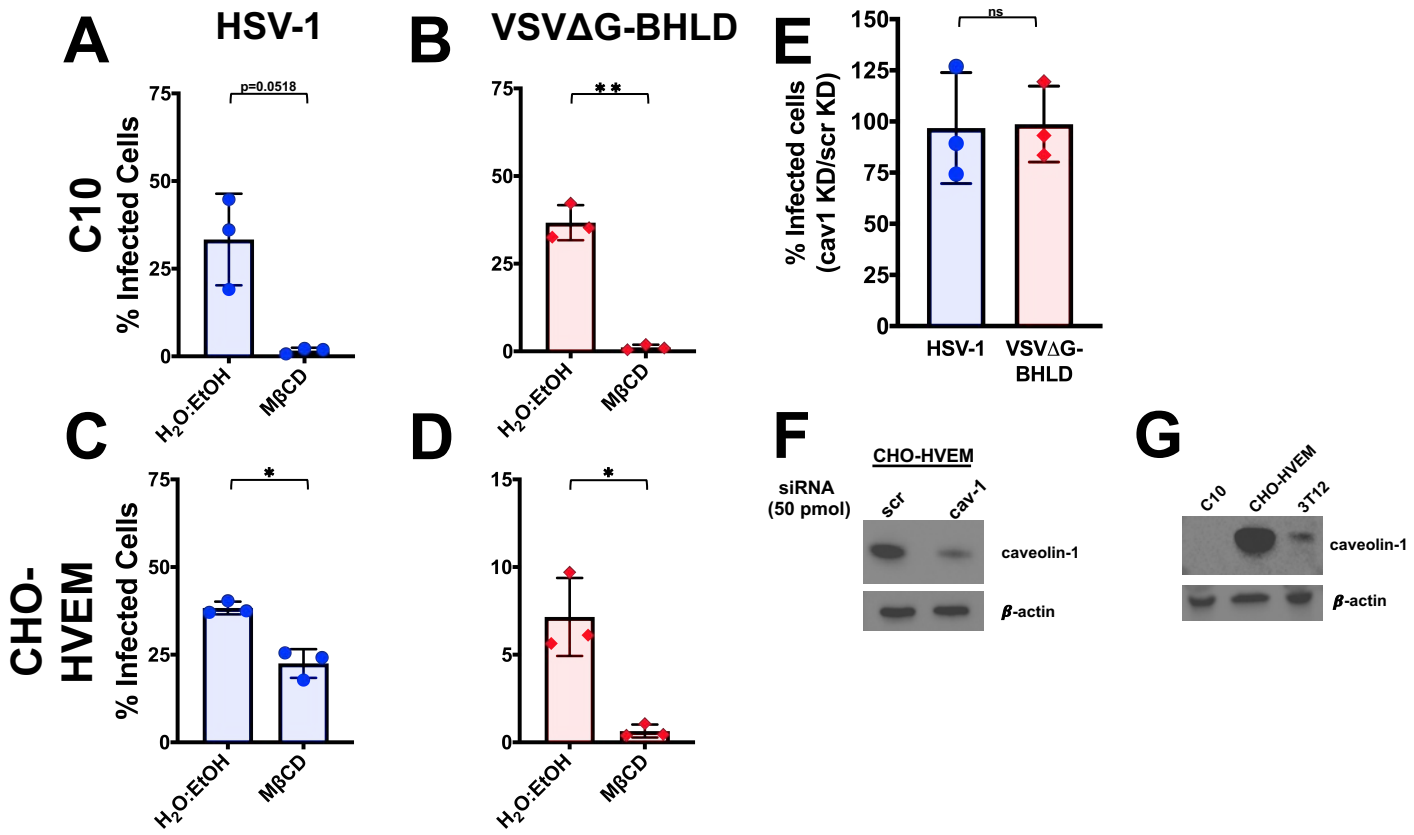

Fig. 8. HSV-1 and VSVΔG-BHLD entry requires cellular cholesterol but not caveolin-1. C10 (A and B) and CHO-HVEM (C and D) cells were pretreated with a cholesterol-removal drug methyl-β-cyclodextran, MβCD (5 mM) and infected with HSV-1 or VSVΔG-BHLD at MOI = 1. Infectivity was quantitated by flow cytometry at 6 hours post infection. E) CHO-HVEM cells were transfected with a caveolin-1 siRNA (cav-1) or a scrambled control siRNA (scr) (both 50 pm) and infected with HSV-1 or VSVΔG-BHLD at MOI = 1. Infectivity was quantitated by flow cytometry at 6 hours post infection. F) Western blot analyses, using antibody clone 4H312 (Santa Cruz Biotechnology), of caveolin-1 knockdown in CHO-HVEM cells (representative of three western blots, one from each biological replicate). G) Western blot analyses, using antibody clone 4H312 (Santa Cruz Biotechnology), of caveolin-1 levels in C10, CHO-HVEM, and 3T12 cells. Significance was calculated using a two-tailed Student's T-test with Welch's correction ($p < 0.05$ = *; $p < 0.01$ = **; $p < 0.001$ = ***).

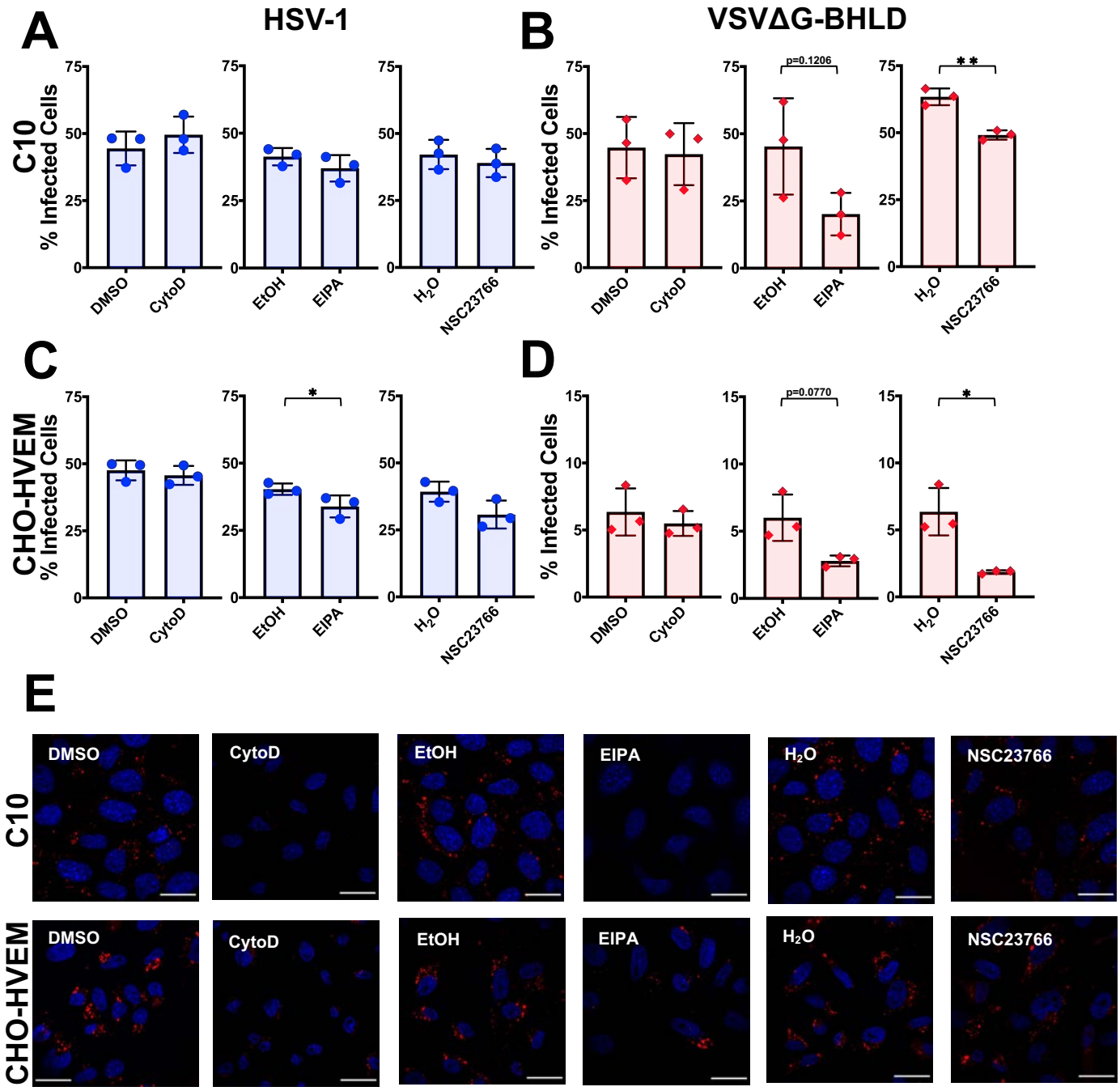

Fig. 9. Neither HSV-1 nor VSVΔG-BHLD entry requires macropinocytosis. C10 (A and B) and CHO-HVEM (C and D) cells were pretreated with macropinocytosis inhibitors cytochalasin D (2 μM), EIPA (25 μM), or NSC23766 (200 μM) and infected with HSV-1 or VSVΔG-BHLD at MOI = 1. Infectivity was quantitated by flow cytometry at 6 hours post infection. Significance was calculated using a two-tailed Student's T-test with Welch's correction (ns = not significant; $p < 0.05$ = *; $p < 0.01$ = **; $p < 0.001$ = ***). E) C10 and CHO-HVEM cells were pretreated with macropinocytosis inhibitors cytochalasin D, EIPA, or NSC23766 at the same concentrations as in panels A-D and then incubated with 1.0 mg/ml of Rhodamine-B-labeled 70-kDa dextran. Cells were fixed, counterstained with DAPI, and imaged by confocal microscopy. Scale bar = 25 μm.

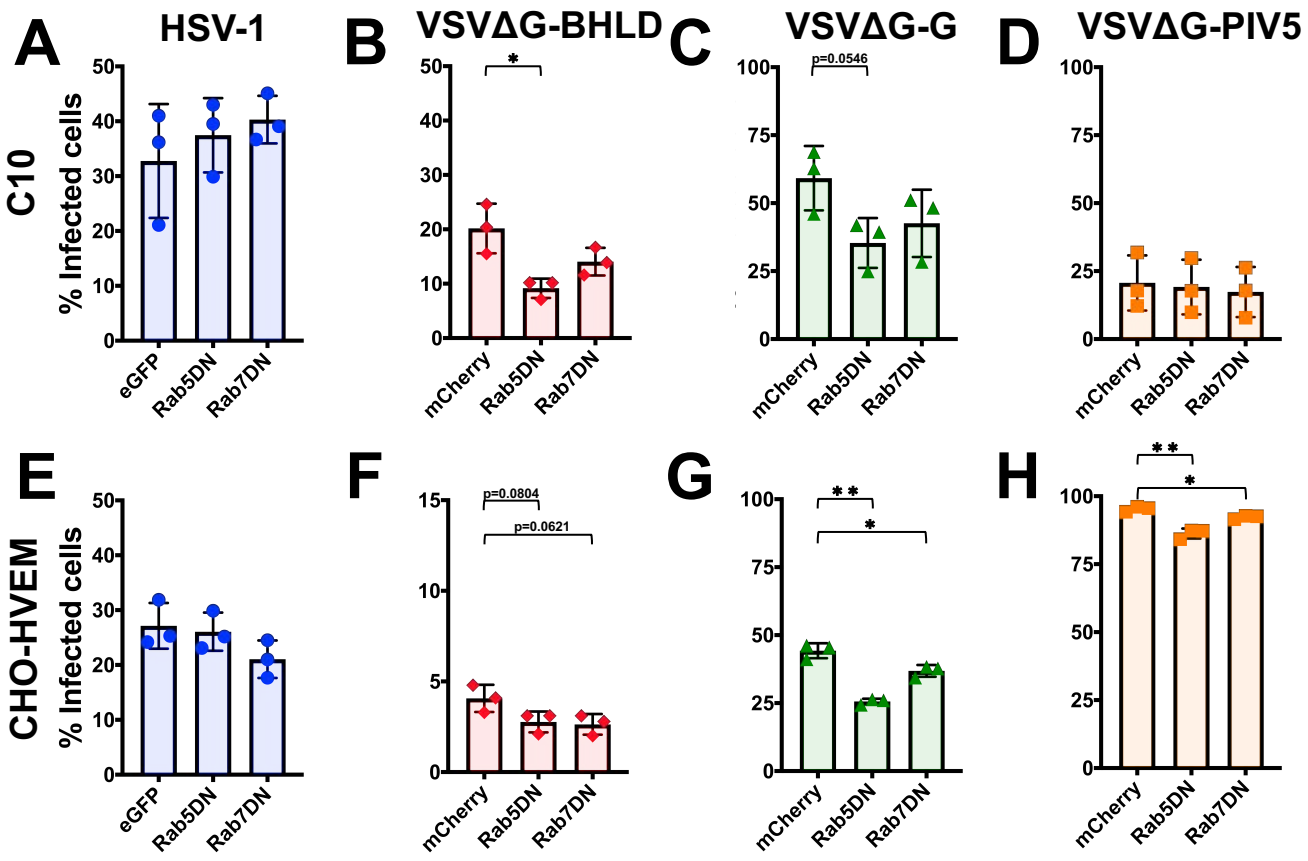

Fig. 10. Rab5 and Rab7 GTPases are dispensable for HSV-1 but not VSVΔG-BHLD entry. C10 (A-D) and CHO-HVEM (E-H) cells were transfected with Rab5DN, Rab7DN, or appropriate empty vector controls (eGFP or mCherry), and infected with HSV-1, VSVΔG-BHLD, VSVΔG-G, or VSVΔG-PIV5 at MOI = 1. Infectivity was quantitated by flow cytometry at 6 hours post infection. Significance was calculated using a two-tailed Student's T-test with Welch's correction ($p < 0.05$ = *; $p < 0.01$ = **; $p < 0.001$ = ***).

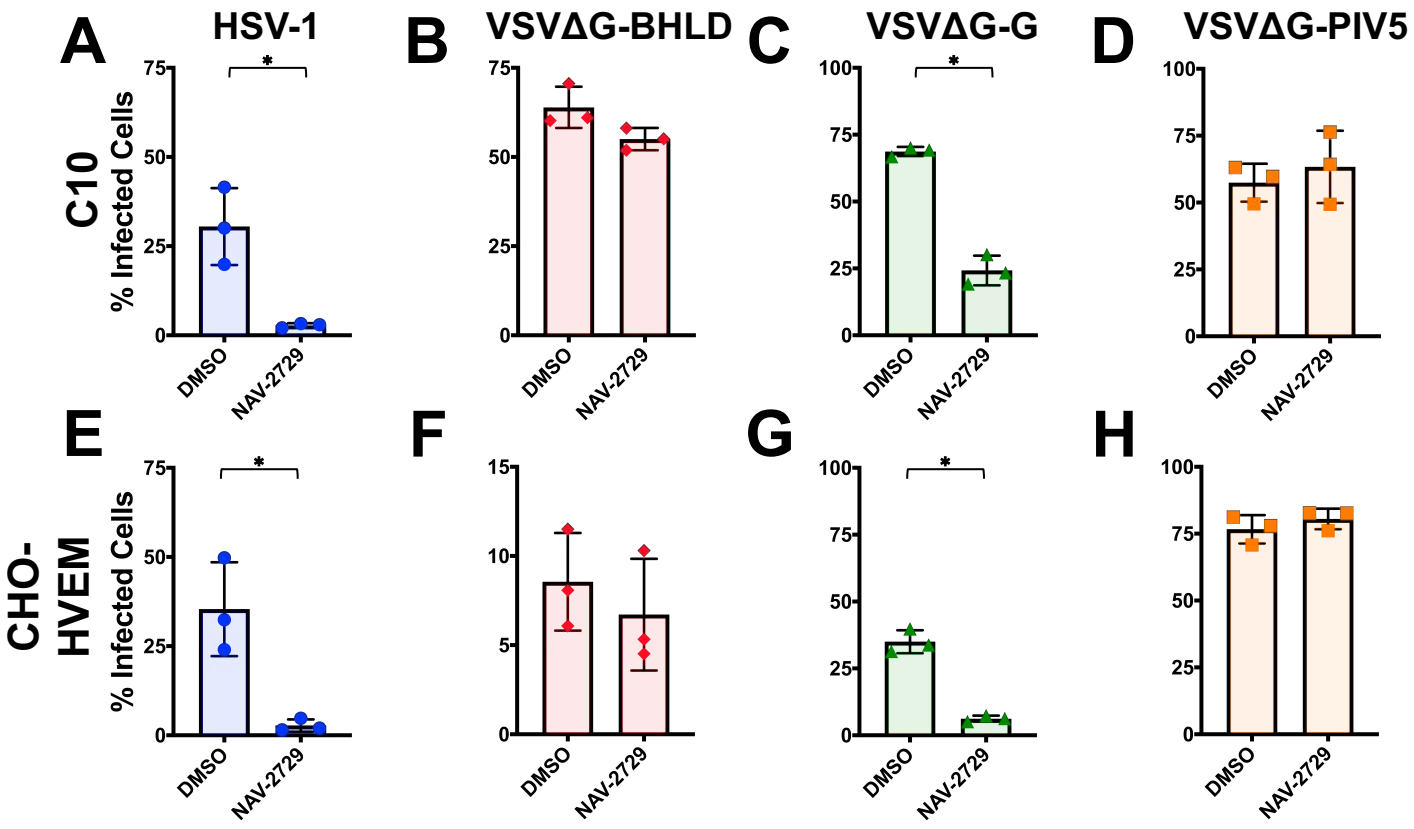

Fig. 11. HSV-1 but not VSVΔG-BHLD entry requires Arf6. C10 (A-D) and CHO-HVEM (E-H) cells were pretreated with the Arf6 inhibitor NAV-2729 (25 μM) and infected with HSV-1 or VSVΔG-BHLD at MOI = 1. Infectivity was quantitated by flow cytometry at 6 hours post infection. Significance was calculated using a two-tailed Student's T-test with Welch's correction ($p < 0.05$ = *; $p < 0.01$ = **; $p < 0.001$ = ***).

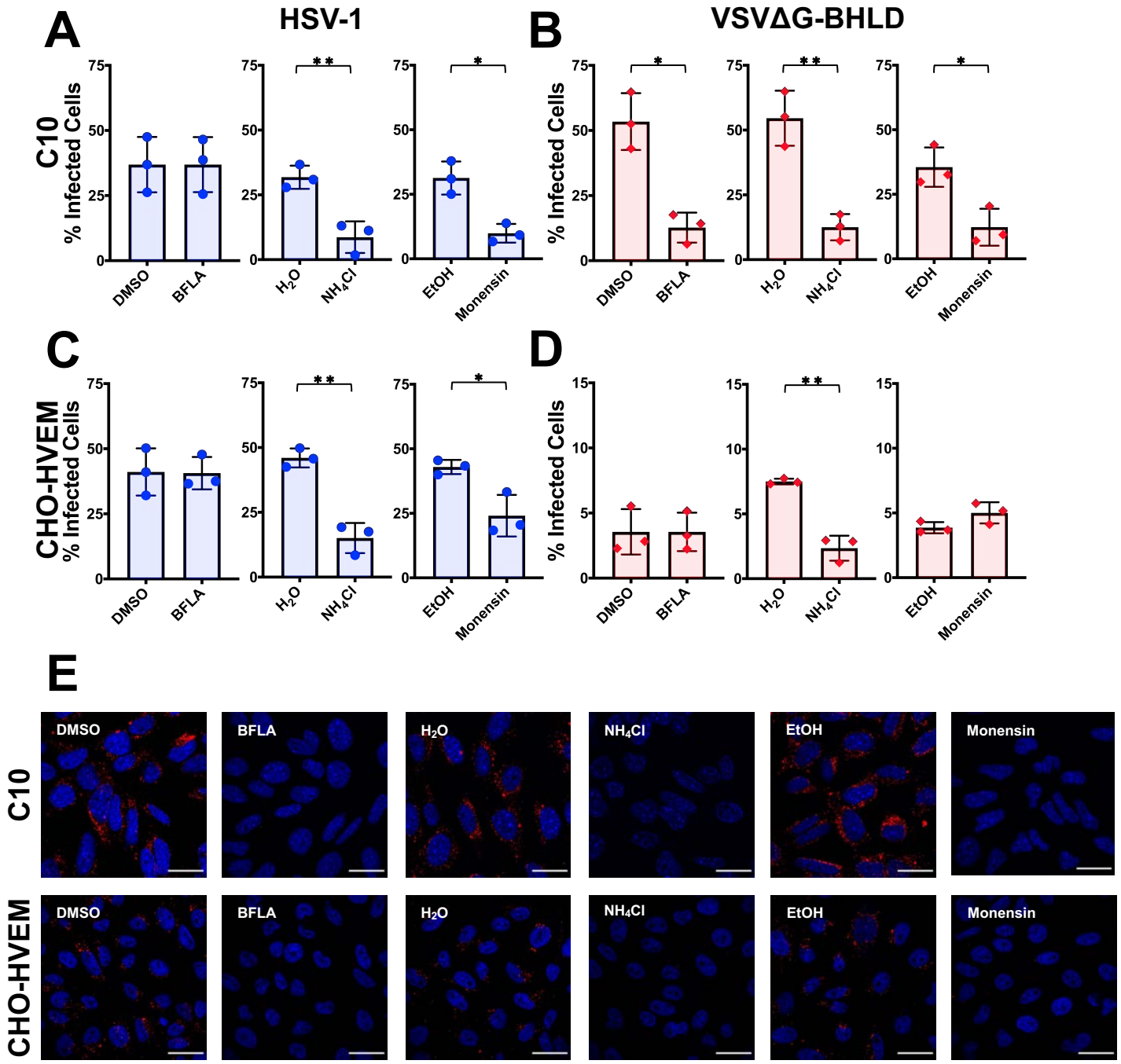

Fig. 12. VSVΔG-BHLD but not HSV-1 entry requires endosomal acidification. C10 (A and B) and CHO-HVEM (C and D) cells were pretreated with inhibitors of endosomal acidification BFLA (100 nM), NH_4Cl (50 mM), or monensin (15 μM) and infected with HSV-1 or VSVΔG-BHLD at MOI = 1. Infectivity was quantitated by flow cytometry at 6 hours post infection. Significance was calculated using a two-tailed Student's T-test with Welch's correction ($p < 0.05$ = *; $p < 0.01$ = **; $p < 0.001$ = ***). E) C10 and CHO-HVEM cells were pretreated with inhibitors of endosomal acidification at the same concentrations as in panels A-D (BFLA, NH_4Cl, or monensin) and then incubated with Lysotracker (1 μM). Cells were fixed, counterstained with DAPI, and imaged by confocal microscopy. Scale bar = 25 μm.

A

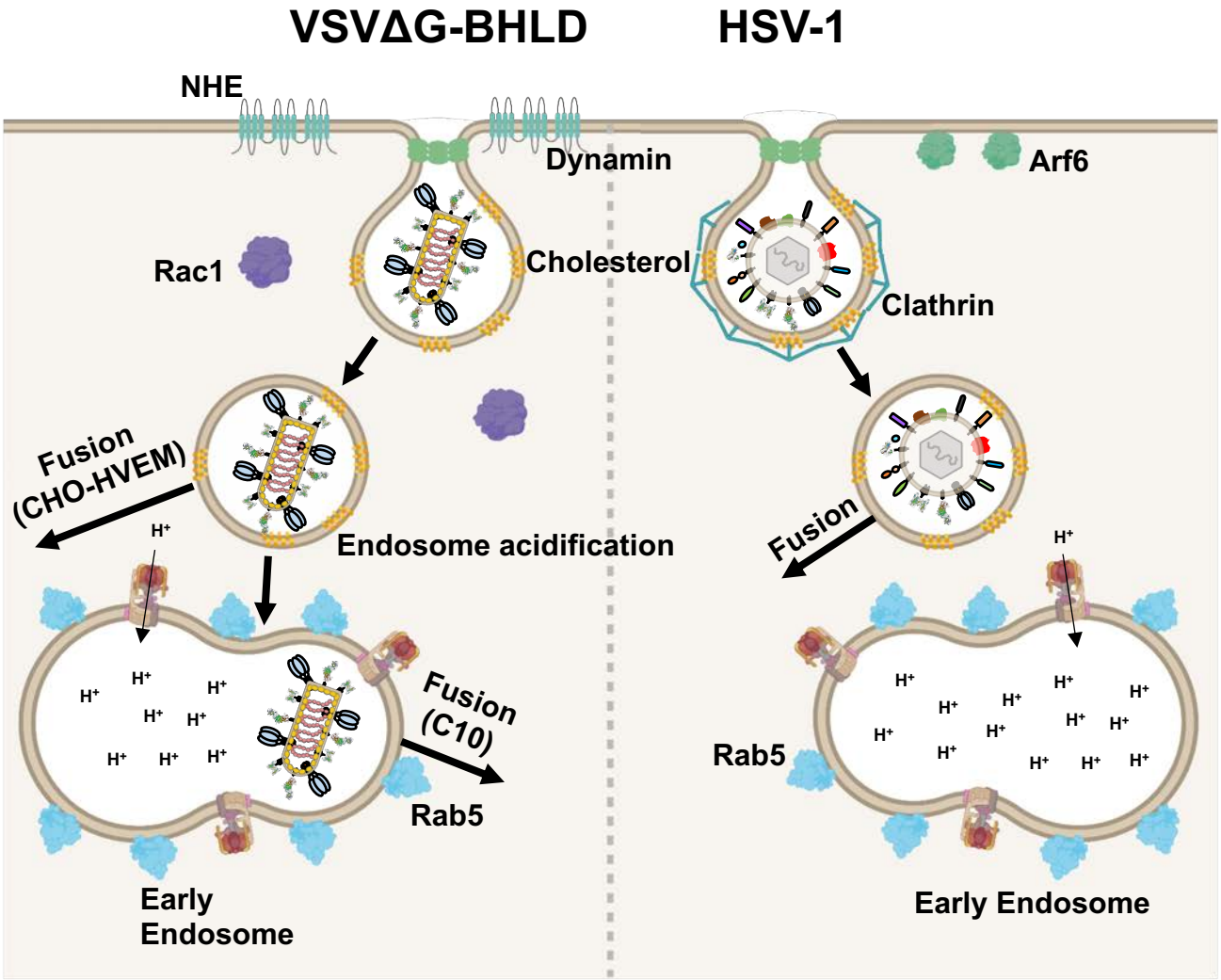

B

		Endocytosis	Dynamin	Clathrin	Cholesterol	Caveolin	Macropino -cytosis	Small GTPases	pH
C10	HSV-1	✓	✓	✓	✓	X	X	Arf6 ✓ Rab5/7 X	X
C10	VSV-BHLD	✓	✓	X	✓	X	X	Arf6 X Rab5/7 ✓	✓
CHO-HVEM	HSV-1	✓	✓	✓	✓	X	X	Arf6 ✓ Rab5/7 X	X
CHO-HVEM	VSV-BHLD	✓	✓	X	✓	X	X	Arf6 X Rab5/7 X	X

Fig. 13. Entry model of VSVΔG-BHLD and HSV-1. A) Entry of VSVΔG-BHLD and HSV-1 entry into C10 and CHO-nectin-1 cells occurs by endocytosis and requires dynamin and cholesterol. VSVΔG-BHLD entry into C10 and CHO-nectin-1 cells additionally requires NHE and Rac1 activity whereas HSV-1 does not. VSVΔG-BHLD entry into C10 cells, but not CHO-nectin-1 cells also requires Rab5 and endosomal acidification. HSV-1 does not require either Rab5 or endosomal acidification for entry into either cell type. B) Table summarizing the cellular molecules important for HSV-1 and VSVΔG-BHLD entry into C10 and CHO-HVEM cells.